Challenges for Developing Rechargeable Room-Temperature Sodium Oxygen Batteries

Bing Sun,* Constantin Pompe, Saustin Dongmo, Jinqiang Zhang, Katja Kretschmer, Daniel Schröder, Jürgen Janek,* and Guoxiu Wang*

The development of high energy-density and low-cost energy storage devices requires new chemistry beyond the horizon of current state-of-the-art lithium-ion batteries. Recently, sodium/oxygen (Na/O_2) batteries have attracted great attention as one possible battery type among the new generation of rechargeable batteries. They convince with superior energy density, a relatively simple cell reaction, and abundance of sodium. Research on Na/O_2 batteries has progressed quickly in recent years. However, a fundamental understanding underpinning the complex chemical/electrochemical side reactions is still insufficient, and many challenges remain unsolved for real practical applications. Herein, recent achievements and remaining issues for the development of rechargeable Na/O_2 batteries are summarized. The discussion focuses on cell reaction mechanisms as well as cathode materials, sodium anodes, and electrolytes as key components of this type of battery. Furthermore, perspectives for future research and technological advances of Na/O_2 batteries are outlined.

1. Introduction

To decelerate global climate change, "carbon neutrality" was proposed at the climate conference to reduce greenhouse gas emissions (Conference of Parties 23, "COP 23"; 2017 in Bonn, Germany).[1] It is widely accepted that global warming and air pollution are mainly caused by greenhouse gas emissions, owing to the consumption of fossil fuels (oil, gas, and coal) for transportation and electricity generation.[1,2] Therefore, moving ground transportation toward electrical propulsion and shifting electricity production from burning of fossil fuels to renewable energy sources can alleviate planetary climate change. The transition to road electrification is currently underway with electric vehicles (EVs) being produced on an appreciable scale annually. Lithium-ion batteries (LIBs) with electric motors are now used as alternative power sources to replace internal combustion engines having a fuel tank. Even though state-of-the-art lithium-ion batteries can deliver driving ranges beyond 300 miles, e.g., guaranteed by Tesla Inc., this range might not be sufficient for all applications. For example, when pulling a loaded trailer, which is a quite common scenario for gasoline-powered cars, ranges nowadays barely exceed 100 miles. Thus, new cell reactions, materials and technologies are required to develop next-generation energy storage systems beyond lithium-ion batteries.[3,4]

Recently, high-energy density alkali metal/air (or alkali metal/oxygen) batteries have been considered as alternative power sources for EVs.[5,6] A typical alkali metal/oxygen battery is a device coupling an alkali metal anode with a porous cathode that utilizes oxygen as the cathode active material.[3] Since oxygen does not need to be stored in the battery, Na/O_2 batteries possess a very high gravimetric energy density in theory. Among various alkali metal/oxygen systems, lithium/oxygen (Li/O_2) batteries exhibit the highest theoretical specific energies. Considering the weight of the discharge product Li_2O_2, Li/O_2 cells operate at up to 2.96 V with a theoretical energy density of 3458 Wh kg^{-1}, that is, several times higher than the energy density of LIBs. However, low energy efficiency (large charge/discharge overpotential > 1 V) and complex side reactions are major obstacles.[7] Electrocatalysts must be added to the cathodes or into electrolytes to reduce the overpotential, and pure oxygen is required, as N_2, CO_2, or H_2O interfere negatively with the cell reactions.[8,9] Furthermore, lithium is not regarded as an abundant element and is unevenly distributed worldwide. The materials cost for LIBs rose rapidly during the first decade of this century, even though their cost on cell levels has slightly decreased due to mass production.[10]

Compared to lithium, sodium/oxygen (Na/O_2) batteries showed higher round-trip efficiencies with pure carbon cathodes. The theoretical energy densities of Na/O_2 cells are calculated to be 1605 Wh kg^{-1} (E^0 = 2.33 V) and 1108 Wh kg^{-1} (E^0 = 2.27 V), considering the discharge products to be Na_2O_2

Dr. B. Sun, Dr. J. Zhang, Dr. K. Kretschmer, Prof. G. Wang
Centre for Clean Energy Technology
University of Technology Sydney
Broadway, Sydney, NSW 2007, Australia
E-mail: bing.sun@uts.edu.au; guoxiu.wang@uts.edu.au
Dr. C. Pompe, Dr. S. Dongmo, Dr. D. Schröder, Prof. J. Janek
Center for Materials Research (LaMa)
Justus Liebig University Giessen
Heinrich-Buff-Ring 16, 35392 Gießen, Germany
E-mail: juergen.janek@phys.chemie.uni-giessen.de
Dr. C. Pompe, Dr. S. Dongmo, Dr. D. Schröder, Prof. J. Janek
Institute of Physical Chemistry
Justus Liebig University Giessen
Heinrich-Buff-Ring 17, 35392 Gießen, Germany

The ORCID identification number(s) for the author(s) of this article can be found under https://doi.org/10.1002/admt.201800110.

**ADVANCED
SCIENCE NEWS**

www.advancedsciencenews.com

**ADVANCED
MATERIALS
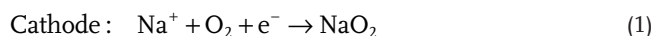TECHNOLOGIES**

www.advmattechnol.de

and NaO_2, respectively.[11] In addition, sodium is the 4th most abundant element in the earth's crust and in seawater. Hence rechargeable Na/O_2 batteries have attracted growing interest as alternative power sources for large scale energy storage.[6,12–14] In an initial study on Na/O_2 batteries by Peled et al., cells working at high temperature (>98 °C) were reported as an alternative battery system to Li/O_2 batteries.[15] Later, a rechargeable Na/O_2 cell working at room-temperature was introduced by Sun et al. with Na_2O_2 as discharge product.[16] Then, Hartmann et al. reported a room-temperature Na/O_2 battery, with NaO_2 as discharge product, that could be cycled with a much lower charge overpotential and better rechargeability than otherwise identical Li/O_2 batteries.[11] Since then, the electrochemical performance of Na/O_2 batteries has been gradually improved through the development of electrode materials and new electrolytes.[17]

Owing to the relatively simple configuration and safety concerns, most researchers focus on nonaqueous electrolyte systems. A rechargeable nonaqueous Na/O_2 battery consists of a Na metal anode and an oxygen electrode (cathode) made of porous conductive materials that draw oxygen from the atmosphere. Although significant advances have been achieved in the past few years, many technological challenges remain unsolved at the current time. In this progress report, we review Na/O_2 batteries and discuss the key remaining challenges for the development of next-generation high energy efficiency and high energy density Na/O_2 batteries, including reaction mechanisms, oxygen electrodes (cathodes), Na metal anodes, and electrolytes.
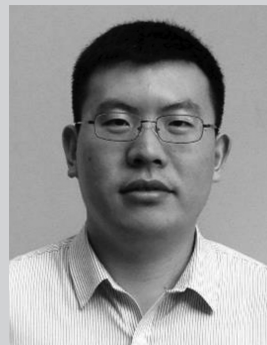
2. Reaction Mechanisms

The rechargeable nonaqueous Na/O_2 battery consists of a Na metal anode and a porous oxygen electrode (cathode), as illustrated in **Figure 1**. During the discharge, a reduction reaction occurs at the porous oxygen electrode, in which the oxygen is reduced to anionic oxygen species. Meanwhile, an oxidation reaction occurs at the anode, in which sodium metal is oxidized to sodium ions. Then, sodium ions migrate to the cathode through a separator and electrolyte and react with oxygen species to form solid sodium oxides (e.g., NaO_2) as shown in Figure 1. During the subsequent charge process, the reverse reaction proceeds, in which sodium ions are reduced to sodium metal and plated on the anode and oxygen is released at the cathode through the decomposition of sodium oxides.[18]

Unlike nonaqueous Li/O_2 cells, where Li_2O_2 has been widely reported as the sole discharge product, different discharge products, e.g., NaO_2 and Na_2O_2, have been identified by different groups often simultaneously forming in Na/O_2 cells (**Table 1**).[19–21] The possible reactions of Na/O_2 cells during discharge are listed in the following chemical equations

$$\text{Cathode:} \quad Na^+ + O_2 + e^- \rightarrow NaO_2 \tag{1}$$

$$\text{Anode:} \quad Na \rightarrow Na^+ + e^- \tag{2}$$

$$\text{Overall:} \quad Na + O_2 \rightarrow NaO_2 \tag{3}$$

or

Bing Sun received his bachelor's degree (2005) and master's degree (2007) from Harbin Institute of Technology (HIT), China and completed his Ph.D. under the supervision of Prof. Guoxiu Wang in 2012 at University of Technology Sydney (UTS), Australia. Currently, he is a senior research fellow in the Centre for Clean Energy Technology at UTS. His current research interests focus on the synthesis and characterization of nanomaterials and their applications in energy storage devices beyond lithium ion batteries.

Jürgen Janek is professor of physical chemistry at Justus Liebig University Giessen (Germany) and scientific director of BELLA (Batteries and Electrochemistry Laboratory), a joint lab of BASF SE and KIT in Karlsruhe (Germany). He received his doctoral degree in chemistry from University of Hannover and was visiting professor at Seoul National University, Tohuku University/Sendai and Université d'Aix-Marseille. His research spans from fundamental studies on electrode kinetics, interface phenomena to plasma electrochemistry and in situ studies for electrochemical cells. Current key interests include new materials and their reactions in lithium solid state batteries, lithium-, and sodium-based next-generation batteries.

Guoxiu Wang is the director of the Centre for Clean Energy Technology and a Distinguished Professor at University of Technology Sydney (UTS), Australia. He is an expert in materials chemistry, electrochemistry, energy storage and conversion, and battery technologies. His research interests include lithium-ion batteries, lithium–air batteries, sodium-ion batteries, lithium–sulfur batteries, supercapacitors, hydrogen storage materials, fuel-cells, graphene, and chemical functionalization of graphene.
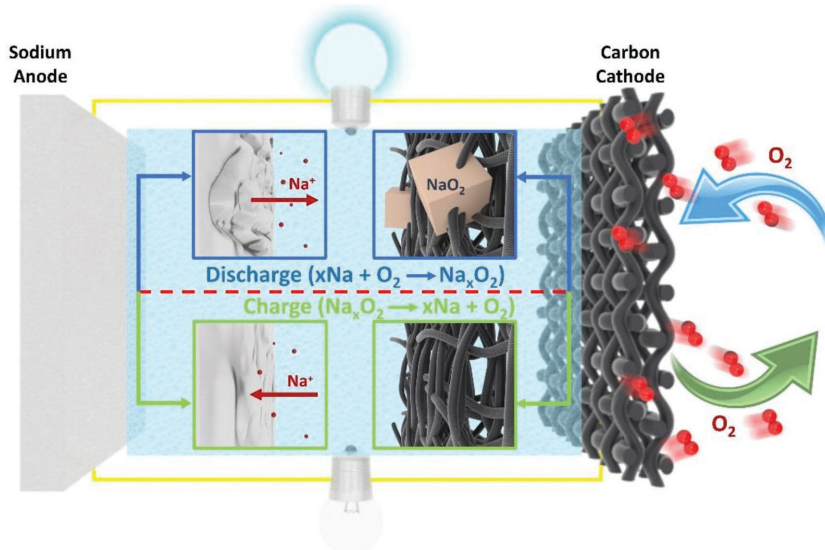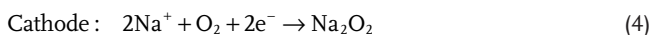
1800110 (2 of 18)

**ADVANCED
SCIENCE NEWS**
www.advancedsciencenews.com

**ADVANCED
MATERIALS
TECHNOLOGIES**
www.advmattechnol.de

Figure 1. Schematic structure illustration and working principle of a typical rechargeable non-aqueous Na/O$_2$ battery.

$$\text{Cathode}: \quad 2Na^+ + O_2 + 2e^- \rightarrow Na_2O_2 \tag{4}$$

$$\text{Anode}: \quad Na \rightarrow Na^+ + e^- \tag{5}$$

$$\text{Overall}: \quad 2Na + O_2 \rightarrow Na_2O_2 \tag{6}$$

So far, despite several attempts, there is no conclusive explanation describing the different reaction pathways for the formation of the different sodium oxides reported. In many studies, NaO$_2$ is the sole discharge product,[11,20,22–34] while the formation of Na$_2$O$_2$ and its hydrates were identified in other studies (Table 1).[16,35–41] From thermodynamic data stated by Bender et al., the free enthalpy for the formation of Na$_2$O$_2$ ($\Delta_r G_{Na_2O_2} = -449.7$ kJ mol^{-1}) is slightly larger than that for the formation of NaO$_2$ ($\Delta_r G_{NaO_2} = -437.5$ kJ mol^{-1}), both at standard pressure and 298 K.[22] The small difference in free enthalpy of only -12.2 kJ mol^{-1} makes it difficult to decide unequivocally whether the peroxide is thermodynamically more stable than the superoxide. For instance, Kang et al. indicated in a theoretical study that the crystallite size of sodium oxides could determine their thermodynamic stability due to the competition between surface and bulk energy.[42] Although bulk Na$_2$O$_2$ appears to be stable and bulk NaO$_2$ is metastable under standard conditions ($P_{O_2} = 1$ atm and $T = 298$ K), nanoscale NaO$_2$ with decreased surface energy appears to be considerably more stable than Na$_2$O$_2$ of equal size, which leads to a reduced nucleation energy. The kinetics of discharge product formation are reported in detail by Yadegari et al.[43]

In addition, studies on Na/O$_2$ cells by different groups were conducted with varied cell configurations and components, making it difficult to identify the control parameters for different reaction pathways.[18] A recent experimental comparison reported by Bi et al. highlighted the importance of cell design for Na/O$_2$ cells (**Figure 2**).[44] By using exactly the same anode, cathode, electrolyte and oxygen gas supply, they obtained different discharge products from two different cell setups. Superoxide-based product (NaO$_2$) was identified by high-energy X-ray diffraction (HE-XRD) and Raman spectroscopy as the sole discharge product in a stainless-steel (SS) cell (Figure 2a,c), while peroxide-based product was observed as the sole discharge product in a glass chamber (GC) cell (Figure 2b,d). The GC cell was sealed by vacuum-grease, which might cause a small amount of air leakage, which in turn might have led to the formation of peroxide. Despite their very systematic study on cell configuration, no definitive answer on the reaction mechanism could be given.

To date, major components of Na/O$_2$ cells such as cathode and electrolyte have been extensively investigated and showed significant influence on the formation of final discharge products as listed in Table 1. For cathodes, different discharge products were obtained using various carbon-based cathode materials.[11,21,35,43,45] The addition of catalysts was able to promote the disproportion reaction (Equation (2)) that leads to the formation of sodium peroxide.[36,37,46,47] For the organic electrolytes, water, and other impurities acting as proton sources appear to play crucial roles to change the reaction pathways and the growth mechanism of discharge products.[26]

So far, it remains unclear what essential factors favor the two-electron reaction for the formation of peroxide instead of the one-electron reaction for the formation of superoxide. Thus, this phenomenon should be addressed with priority for the development of high performance Na/O$_2$ batteries.

3. Oxygen Electrodes

The specific capacity of nonaqueous Na/O$_2$ batteries is determined by the quantity of insoluble discharge products stored in the porous oxygen electrode after discharge. During the discharge process, most of the pores inside the oxygen electrodes are gradually filled with the solid discharge products (i.e., NaO$_2$, Na$_2$O$_2$), which blocks the diffusion pathways for O$_2$ and electrolyte transfer and induces the termination of the discharge process. The accumulation of the insoluble discharge products during deep discharge also causes volume expansion of the oxygen electrode. After the removal of the discharge products during the subsequent charge process, the conductive electrode materials of the oxygen electrodes inevitably become less interconnected, which causes deterioration of the oxygen electrode. Therefore, the final electrochemical performance of the Na/O$_2$ cell is strongly dependent on the capability of the oxygen electrode. An ideal oxygen electrode must possess several key characteristics, including high electrical conductivity, high surface area with appropriate porous structure, effective catalytic activity to promote the oxygen reduction reaction (ORR) and oxygen evolution reaction (OER), and sufficient mechanical

1800110 (3 of 18)

Table 1. A summary of various reported discharge products of Na/O$_2$ cells.

Year	Author	Major discharge product	Electrolyte	Oxygen electrode
2013	Hartmann[11,27]	NaO$_2$	0.5 M NaOTf in diglyme	GDL H2315
2014	McCloskey[23]	NaO$_2$	0.2 M NaOTf in DME	P50 Avcarb carbon paper
2014 2015	Bender[22,48]	NaO$_2$	0.5 M NaOTf in diglyme	GDL H2315; SFG-44; Super PLi; Ketjenblack EC 600JD; HSAG 500; SCR-1; CNTs
2014	Zhao[21]	NaO$_2$	0.5 M NaOTf in tetraglyme	Vertically aligned carbon nanotubes (VACNTs)
2015	Bi[28]	NaO$_2$	0.5 M NaOTf in diglyme	P50 Avcarb carbon paper
2015	Xia[26]	NaO$_2$	0.5 M NaOTf in diglyme	GDL H2315
2015	Ortiz-Vitoriano[24]	NaO$_2$	0.1 M NaClO$_4$ in DME	Vertically aligned carbon nanotube carpets
2016	Abate[25]	NaO$_2$	1 M NaOTf in DME	P50 Avcarb carbon paper
2016	Aldous[20]	NaO$_2$	0.1 M NaOTf in DMSO or DMA	Au
2016	Black[49]	NaO$_2$	0.5 M NaOTf in diglyme	^{13}C carbon
2016	He[29]	NaO$_2$	0.9–4.1 M NaTFSI in DMSO	GDL H2315
2016	Kim[30]	NaO$_2$	0.5 M NaOTf in diglyme	Ketjen Black carbon
2016	Liu[31]	NaO$_2$	0.25 M NaClO$_4$ in DME	Reduced graphene oxide
2016	Lutz[32]	NaO$_2$	0.5 M NaOTf in DME, diglyme or tetraglyme	GDL H2315
2017	Liu[33]	NaO$_2$	0.5 M NaOTf in diglyme 0.5 M NaPF$_6$ in diglyme	GDL H2315
2017	Lutz[34]	NaO$_2$	0.5 M NaOTf in diglyme 0.5 M NaPF$_6$ in diglyme 0.5 M NaClO$_4$ in diglyme 0.5 M NaTFSI in diglyme	GDL H2315
2017	Sun[45]	NaO$_2$	0.5 M NaOTf in diglyme	Carbon spheres; Super P
2013	Liu[38]	Na$_2$O$_2$	0.25 M NaPF$_6$ in DME	Graphene
2013	Li[35]	Na$_2$O$_2$	0.5 M NaOTf in diglyme	Nitrogen-doped graphene
2012	Sun[16]	Na$_2$O$_2$	1 M NaPF$_6$ in EC:DMC 1:1	Diamond-like carbon thin film
2014	Liu[36]	Na$_2$O$_2$	1 M NaClO$_4$ in DME	NiCo$_2$O$_4$ nanosheets on Ni foam
2015	Yadegari[39]	Na$_2$O$_2$	0.5 M NaOTf in diglyme	Vertically grown nitrogen doped carbon nanotubes on carbon paper
2015	Hu[37]	Na$_2$O$_2$	1 M NaOTf in tetraglyme	CaMnO$_3$ and Super P
2016	Zhang[50]	Na$_2$O$_2$	0.3 M NaOTf in diglyme	Nitrogen-doped graphene aerogels
2015	Yin[51]	Na$_2$O$_2$	1 M NaClO$_4$ in DME and 0.001 M NaI	CNT on Ni foam
2015	Sun[41]	Na$_2$O$_2$	0.5 M NaOTf in diglyme	Nitrogen-doped carbon nanotubes
2014	Jian[52]	Na$_2$O$_2$·2H$_2$O	0.5 M NaOTf in diglyme 0.5 M NaTFSI in tetraglyme	CNT paper
2013	Kim[53]	Na$_2$O$_2$·2H$_2$O	1 M NaClO$_4$ in PC 1 M NaClO$_4$ in tetraglyme	Ketjenblack
2017	Ma[46]	Na$_2$O$_2$·2H$_2$O	0.5 M NaOTf in tetraglyme	Pd/ZnO/Carbon
2014	Yadegari[43]	NaO$_2$, Na$_2$O$_2$, Na$_2$CO$_3$	0.5 M NaOTf in diglyme	Heat-treated carbon black N330
2016	Ma[54]	NaO$_2$, Na$_2$O$_2$	0.5 M NaOTf in tetraglyme	Nitrogen-doped carbon
2017	Li[55]	NaO$_2$, Na$_2$O$_2$	0.5 M NaOTf in tetraglyme	La$_2$Co$_2$O$_7$ and Super PLi
2017	Sun[47]	NaO$_2$, Na$_2$O$_2$	0.5 M NaOTf in diglyme	Co$_3$O$_4$ decorated carbon nanotubes
2016	Shu[56]	Na$_2$O$_2$, Na$_2$O$_2$·2H$_2$O	1 M NaOTf in tetraglyme	Boron-doped onion-like carbon
2017	Ma[57]	Na$_2$O$_2$, Na$_2$O$_2$·2H$_2$O	0.5 M NaOTf in tetraglyme	N-doped carbon fibers; Co-embedded N-doped carbon fibers

strength to tolerate the volume expansion during the formation and decomposition of the insoluble solid discharge products. In this aspect, major endeavors were devoted into the discovery and application of appropriate cathode materials and catalysts, such as nanostructured carbon materials, heteroatom-doped carbon materials, metal nanoparticles, and transition metal oxides to improve the energy density and cycling life of Na/O$_2$ batteries.
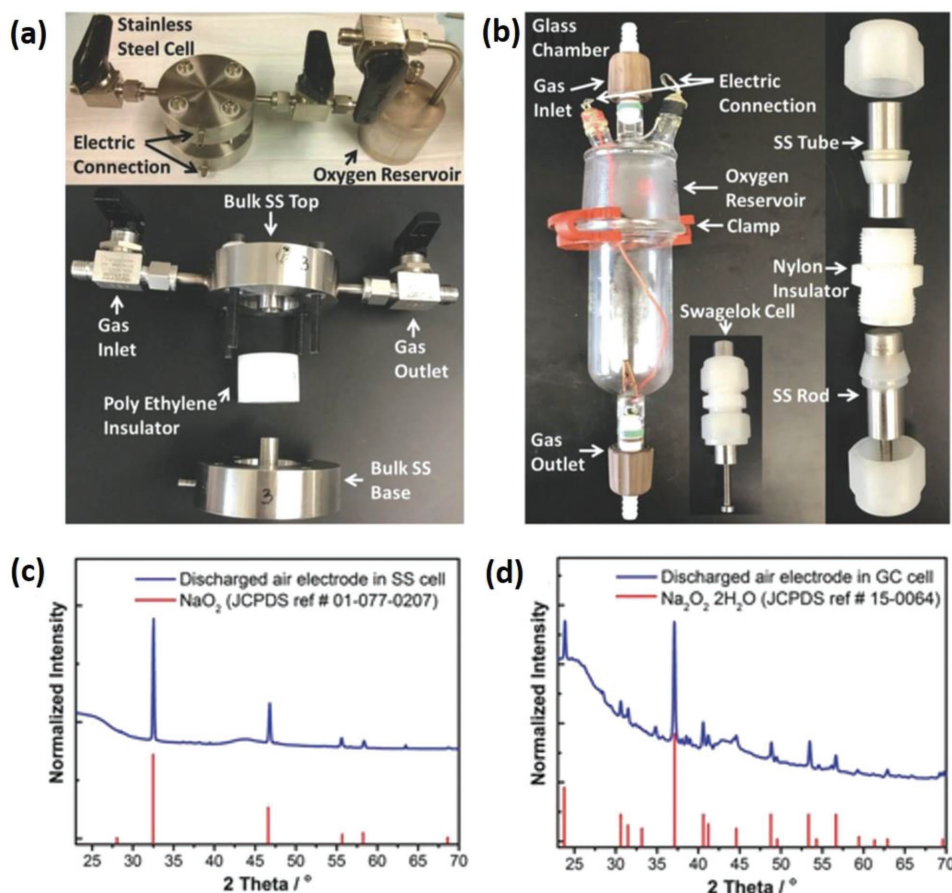
Figure 2. Optical images of a) a stainless-steel (SS) Na/O$_2$ cell, and b) a Swagelok Na/O$_2$ cell sealed in a glass chamber (GC). High-energy X-ray diffraction patterns (HE-XRD) of the discharge product in c) a SS cell and d) a GC cell. Reproduced with permission.[44] Copyright 2017, Wiley-VCH.

3.1. Carbon-Based Oxygen Electrodes

Carbon materials are widely used to prepare oxygen electrodes for metal/air (oxygen) batteries owing to their unique properties such as high electronic conductivity, light weight, low cost, and abundant resources. A number of studies on Na/O$_2$ cells with carbon-based oxygen electrodes were reported recently, such as carbon paper,[11] carbon nanotubes (CNTs),[21,39,41,48,52] graphene,[35,38,50] porous carbon spheres,[45] etc. Application of high surface area carbon materials with optimized nanostructures to improve the discharge capacity and cycling stability became one of the major subjects of study within the Na/O$_2$ battery research field.

3.1.1. Diamond-Like Carbon Thin Film and Carbon Paper

The initial work that demonstrated the possibility of operating a rechargeable Na/O$_2$ cell at room-temperature was first reported by Sun et al. using diamond-like carbon (DLC) thin films (fabricated by radio frequency sputtering) as the oxygen electrode.[16] The Na/O$_2$ cells with nanostructured DLC thin film electrodes in a carbonate-based electrolyte achieved a specific discharge capacity of 1884 mA h g^{-1} at a 0.1 C rate. The

discharge products were identified to be crystallized Na$_2$O$_2$ and amorphous carbonate salts. Later, Hartmann et al. reported a rechargeable room-temperature Na/O$_2$ cell using a carbon-fiber gas diffusion layer (GDL) as the cathode.[11] Unlike in Li/O$_2$ cells, where the discharge capacity of the GDL cathode is negligible even at very low current density, the Na/O$_2$ cell with a GDL cathode achieved a discharge capacity of over 3.3 mA h cm^{-2} (electrode area) in an ether-based electrolyte (0.5 M NaOTf in diglyme) (**Figure 3**a).[11,58,59] An unexpected breakthrough of this work is the lowest charge overpotential ever reported in literature related to Li/O$_2$ or Na/O$_2$ batteries. The discharge product was unequivocally identified to be NaO$_2$ with a macroscopic cubic symmetry morphology (Figure 3c–e), which demonstrated that the ORR occurs as a single-electron transfer process. The kinetically highly favored single-electron transfer reaction should lead to reduced overpotentials during charging.

3.1.2. Carbon Nanotubes

Na/O$_2$ cells with carbon nanotubes (CNTs) as cathode materials have also been intensively investigated. Jian et al. employed a 3D interpenetrating CNT paper as a binder-free oxygen electrode for Na/O$_2$ batteries.[52] The CNT paper achieved an initial
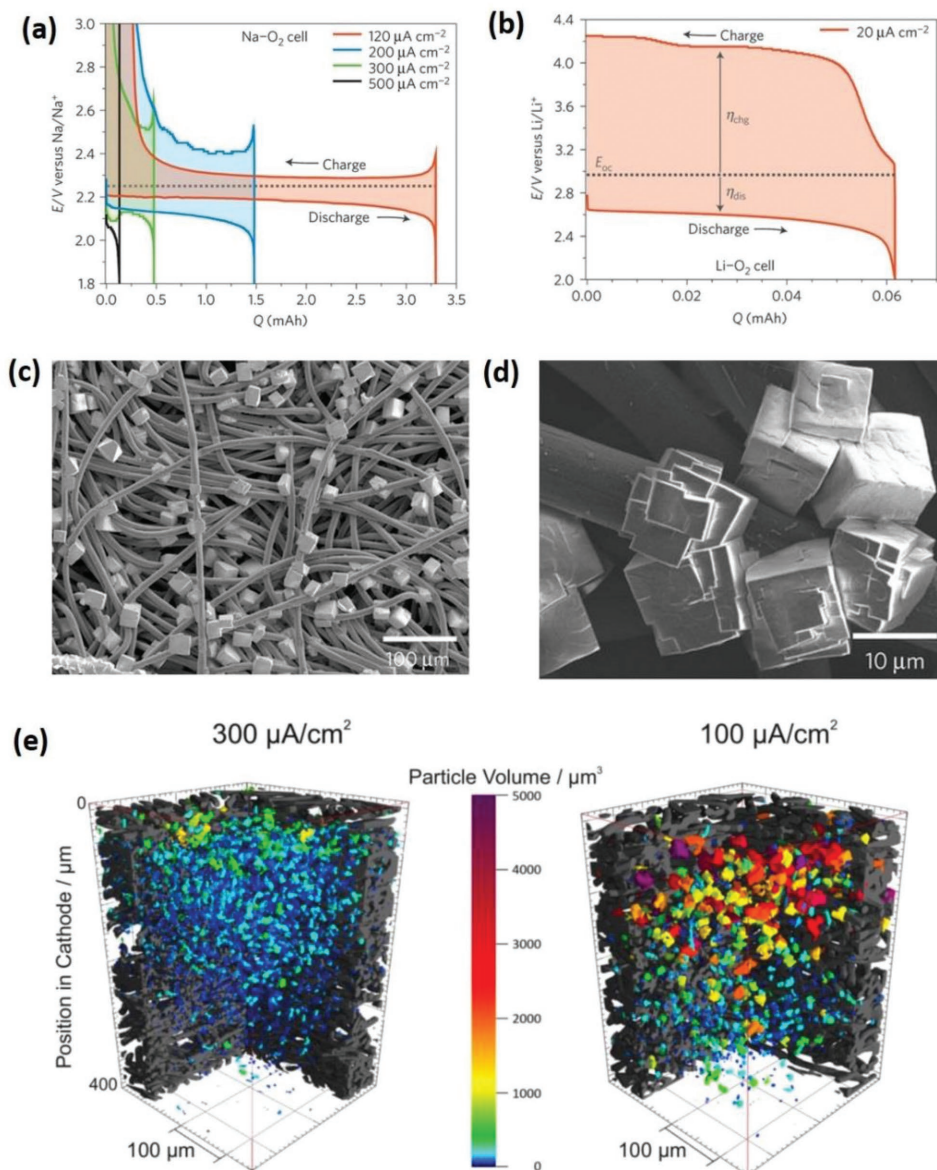
Figure 3. a) Discharge/charge voltage profiles of Na/O$_2$ cells with GDL cathodes at different current densities. b) Discharge/charge voltage profile of a Li/O$_2$ cell with GDL cathodes for comparison. c,d) SEM images of GDL cathode after discharge to 2 mA h at 80 µA cm^{-2}. Reproduced with permission.[11] Copyright 2013, Springer Nature. e) Particle size distribution analysis of selected regions inside the cathodes. Reproduced with permission.[60] Copyright 2013, Springer Nature.

discharge capacity of 7530 mA h g^{-1} in an electrolyte of 0.5 M NaOTf in diglyme and a discharge capacity of 5930 mA h g^{-1} in an electrolyte of 0.5 M NaTFSI in triglyme, respectively, at a current density of 500 mA g^{-1}. The main crystalline discharge product is identified to be Na$_2$O$_2$·2H$_2$O through XRD analysis (Table 1). Zhao et al. also reported a long-life Na/O$_2$ battery with vertically aligned carbon nanotubes (VACNTs) grown on stainless steel mesh as the oxygen electrode.[21] The Na/O$_2$ batteries with VACNT cathode were tested in four atmosphere modes and exhibited remarkably different electrochemical performances, indicating changes in the reaction mechanism. In a static Ar/O$_2$ (80/20 vol%) atmosphere with a cutoff discharge capacity of 750 mA h g^{-1}, the Na/O$_2$ cell with VACNTs was cycled for

more than 100 cycles with a low over-potential (≈200 mV) and a high electrical energy efficiency (90%). Bender et al. further investigated the electrochemical performances of different CNT electrodes in Na/O$_2$ batteries, including pure CNT electrodes, CNT/carbon fiber (CF) mixed electrodes, and CNT/carbon black (CB) mixed electrodes.[48] Of the three different tested electrodes, the pure CNT electrodes achieved the highest discharge capacity of 1530 mA h g^{-1} (4.2 mA h cm^{-2}) at a current density of 0.2 mA cm^{-2}, which is significantly higher than that of their previously reported GDL electrode.[11]

Free-standing nitrogen-doped carbon nanotube (NCNT) electrodes and pristine CNT electrodes were prepared by Sun et al. through a self-stacking method.[41] Na/O$_2$ batteries with NCNT

electrodes delivered a discharge capacity of ≈1887 mA h g^{-1} at a current density of 25 mA g^{-1}, which is higher than those of Na/O$_2$ batteries with pristine CNT electrodes. The enhanced high rate capability and improved cycling stability of NCNT electrodes were attributed to the robust nanostructure of aligned NCNTs and the improved catalytic activity after nitrogen doping. A free-standing oxygen electrode based on vertically grown NCNTs on carbon paper (NCNT-CP) was also reported by the same group.[39] The free-standing NCNT-CP electrodes were prepared using a spray pyrolysis chemical vapor deposition (SPCVD) method and exhibited a hierarchical porous structure. Large micrometer-sized pores formed between the individual carbon fibers, facilitating oxygen and electrolyte transportation. In the meantime, the insoluble discharge products were accommodated inside mesopores provided between the vertically aligned NCNTs. Compared with the CP electrodes, the NCNT-CP electrodes achieved remarkably increased discharge capacities of about 11, 9, and 6 mA h cm^{-2}, at current densities of 0.1, 0.2, and 0.5 mA cm^{-2}, respectively. The elevated discharge capacities and enhanced rate capabilities of the Na/O$_2$ cells with NCNT-CP electrodes are results of the increased specific surface area provided by the vertically-aligned NCNTs for discharge products accommodation and the abundant micrometer-sized pores of CP for oxygen and electrolyte transportation.

3.1.3. Graphene

Graphene materials with a unique 2D structure, super high specific surface area, and excellent electronic conductivity, were intensively studied as cathode materials for Li/O$_2$ batteries.[61,62] Recent studies on Na/O$_2$ cells with graphene nanosheet (GNS) cathodes demonstrated significantly improved electrochemical performance as well. Liu et al. reported the application of graphene in Na/O$_2$ batteries and achieved a high specific capacity of 9268 mA h g^{-1} at a current density of 200 mA g^{-1}.[38] Later, an oxygen electrode made of nitrogen-doped graphene nanosheets (N-GNSs) was reported by Li et al.[35] The N-GNSs oxygen electrode achieved a discharge capacity about two times higher than the oxygen electrode made from bare GNSs. By directly growing nitrogen-doped graphene aerogels (N-GA) on Ni foam, Zhang et al. successfully prepared a 3D binder-free air electrode with a well-preserved porous architecture.[50] Na/O$_2$ cells with 3D N-GA cathodes achieved a much higher capacity than bare graphene aerogel-based cathodes. The improved electrochemical performance of Na/O$_2$ cells with 3D N-GA cathodes was enabled by N-containing functional groups on graphene nanosheets. These functional groups appear to serve as the active sites to promote the ORR and guided the homogenous distribution of the nanoscale discharge products, Na$_2$O$_2$, on graphene nanosheets. The reduction of the particle size of the discharge products was assumed to be beneficial to decrease the charge overpotential.

3.1.4. Other Porous Carbon Materials

A series of porous carbon materials with controlled specific surface area and pore-size distribution were synthesized by Yadegari et al. through treating commercial carbon with corrosive gas at different temperatures.[43] The discharge capacities of the porous carbon-based electrodes were linearly correlated with the surface area and the morphologies of the discharge products were strongly dependent on the specific surface area and pore size distribution of the porous carbon materials. Furthermore, it was found that the chemical composition of discharge products as well as charging overpotential were affected by the discharge current density and both sodium peroxide and superoxide were identified as discharge products.

Recently, Sun et al. reported that hierarchical porous carbon spheres (PCSs) prepared through a facile chemical vapor deposition (CVD) method showed outstanding electrochemical performance as the cathode materials in Na/O$_2$ batteries (**Figure 4**).[45] The oxygen electrodes made of PCSs exhibited hierarchical porous structures that facilitated oxygen diffusion and electrolyte impregnation to the inner part of the electrode. Meanwhile, the discharge product, NaO$_2$, showed a film-like morphology, and conformally deposited on the PCS electrode (Figure 4d,e).

3.2. Catalysts

Inspired by the tremendous preceding studies on catalysts for fuel cells, introducing electrocatalysts to improve the reaction activities of ORR and OER became a widely used strategy to improve the electrochemical performances of alkaline metal-oxygen batteries. Recently, a variety of electrocatalysts were reported in an attempt to increase the energy efficiency and cycling stability of Na/O$_2$ batteries such as metal oxides,[36,37,47,55] metal nanoparticles,[50,57,63] soluble catalysts (i.e., redox mediators),[51,64] and their combinations.[40] However, the mechanisms responsible for the catalytic activity are still in a highly debated status due to the complicated nature of ORR and OER in nonaqueous electrolytes compared to the reactions in aqueous electrolytes. In this section, we summarize some of the recent progress in catalyst research for Na/O$_2$ batteries.

Metal oxides were initially employed to catalyze the ORR and OER for Na/O$_2$ batteries with Na$_2$O$_2$ as discharge product (NaO$_2$ only requires pure carbon materials). NiCo$_2$O$_4$ nanosheets supported on Ni foam as carbon-free and binder-free oxygen cathodes for Na/O$_2$ batteries were first reported by Liu et al. and Na$_2$O$_2$ nanosheets were observed as the major discharge products formed on the free-standing electrode after discharge to 1.8 V (**Figure 5**a,b).[36] Later, Hu et al. reported that porous CaMnO$_3$ microspheres exhibited remarkable electrocatalytic activity both for ORR and for OER (Figure 5c,d), which could be attributed to the unique hierarchical porous structures of the catalysts and the use of the relatively stable ether-based electrolytes.[37] Sun et al. used atomic layer deposition (ALD) technology to synthesized Co$_3$O$_4$ decorated carbon nanotubes (CNT@Co$_3$O$_4$) as cathode catalysts for Na/O$_2$ batteries (Figure 5e,f).[47] Synchrotron-based X-ray analysis demonstrated that the homogeneously dispersed Co$_3$O$_4$ catalyst on CNTs could serve as functionalized active sites to efficiently decompose discharge products, such as sodium peroxide, superoxide, and carbonates. Recently, Li et al. employed a series of pyrochlore-type oxides (La$_{2-x}$Sr$_x$Sn$_2$O$_7$ and La$_2$Sn$_{2-x}$Co$_x$O$_7$)

**ADVANCED
SCIENCE NEWS**
www.advancedsciencenews.com

**ADVANCED
MATERIALS
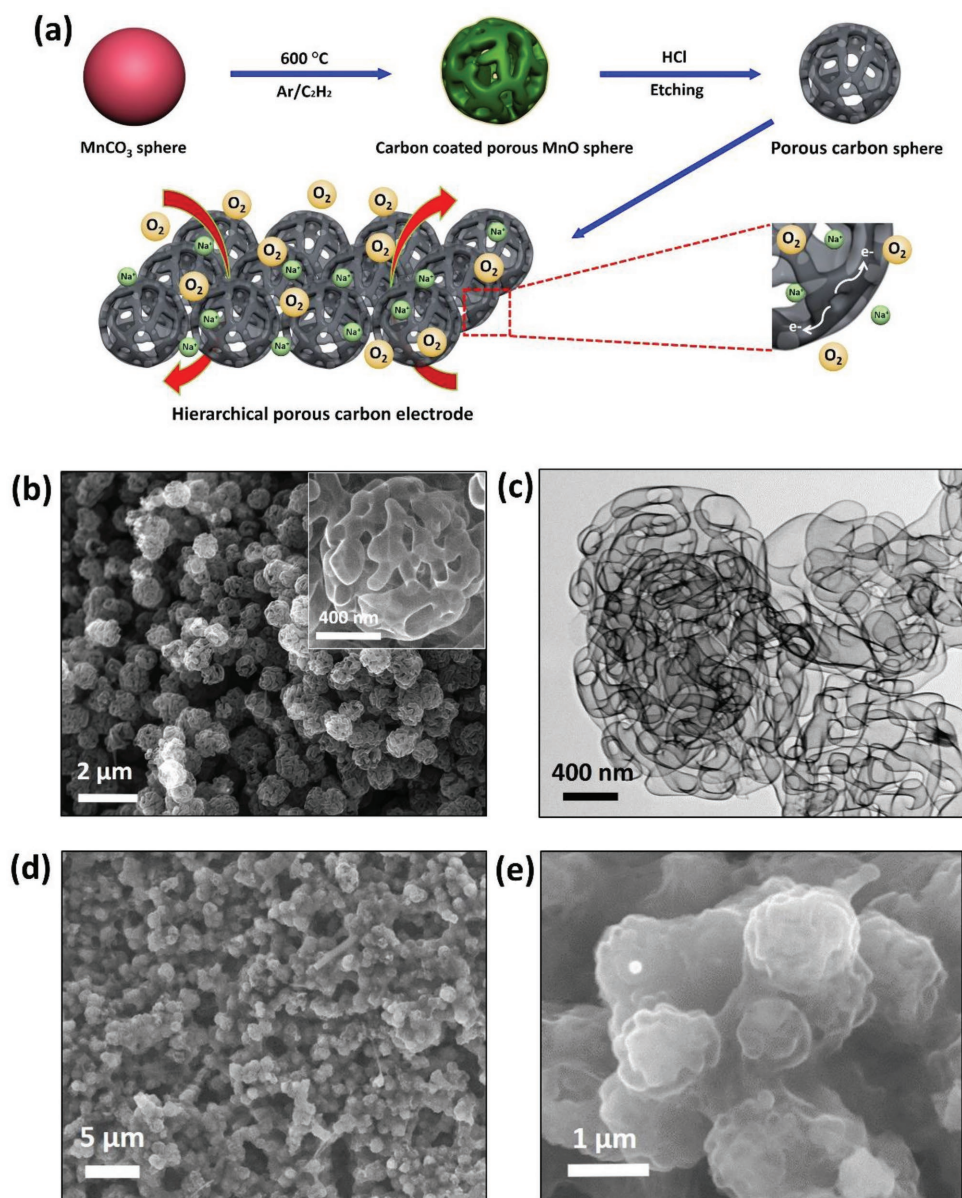TECHNOLOGIES**
www.advmattechnol.de

Figure 4. a) Schematic illustration of the synthesis processes for PCSs and a hierarchical porous oxygen cathode made from PCSs. SEM b) and TEM c) images of as-prepared PCSs. The inset in (b) is a high magnification SEM image of PCSs. d,e) SEM images of discharged PCS electrodes at different magnifications. Reproduced with permission.[45] Copyright 2017, Wiley-VCH.

as model catalysts and discovered that the enhancement of the catalytic activities for ORR and OER in Na/O$_2$ cells was related to the metallic character and the specific surface area of pyrochlore-type oxides (Figure 5e,f).[55]

Metal particles and their combination with nanostructured carbon materials are widely accepted to be excellent electrocatalysts for ORR and OER in the research field of Li/O$_2$ batteries.[65–68] For Na/O$_2$ batteries, platinum nanoparticles uniformly dispersed on graphene nanosheets (Pt@GNSs) and silver nanoparticle-decorated reduced graphene oxide (Ag-RGO) were employed as cathode catalysts for Na/O$_2$ batteries and showed enhanced electrocatalytic activity for cathode reactions.[63,69] Cobalt (Co) nanoparticles embedded in N-doped carbon fibers

(Co-ECNCFs) synthesized through a facile electrospinning technology were reported by Ma et al. (Figure 5i,j).[57] Compared with N-doped carbon fibers (NCFs) electrodes, Na/O$_2$ batteries with Co-ECNCFs cathodes showed increased discharge capacities (increased by ≈57%), reduced charge overpotential (reduced by 200 mV) and notably extended cycle life (tested up to 112 cycles). The enhanced catalytic activity was likely the result of the synergistic effect between N-doped carbon fibers and Co nanoparticles. The interconnected carbon fibers can provide fast electron transfer pathways. The micropores formed between each individual carbon fiber can provide large space for electrolyte and oxygen transportation as well as discharge products accommodation.

By combining the advantages of transition metal oxides and precious metal nanoparticles, a bifunctional solid state catalyst with hierarchical porous structure and high surface area was introduced by Yadegari et al. to catalyze both ORR and OER in Na/O$_2$ and Li/O$_2$ cells (Figure 5k,l).[70] The catalyst was synthesized based on a free-standing graphene foam (Gr) as the substrate. Nitrogen-doped carbon nanotubes (NCNTs) were grown on graphene foam, followed by in situ growth of Mn$_3$O$_4$ on NCNTs, which was denoted as Gr/NCNT/MnO. Finally, an ultrathin layer of Pd was deposited on the surface of as-prepared Gr/NCNT/MnO through an atomic layer deposition (ALD) method to generate the Gr/NCNT/MnO/Pd catalyst. A variety of electrochemical measurements showed that the as-prepared catalysts could significantly enhance catalytic activities in both ORR and OER. The surface defects and hydroxyl functional groups on Mn$_3$O$_4$ nanosheets provide large numbers of reaction sites to promote ORR. Meanwhile, Pd nanoclusters on the surface of Mn$_3$O$_4$ enhanced the charge transfer at the product/electrode interface to catalyze the decomposition of discharge products and reduce the charge overpotential. In addition, detailed XAS studies demonstrated that a higher oxygen-bonding capability of the catalysts may be able to stabilize O$_2$ intermediates on the catalyst surface during the electrochemical reaction and contribute to a higher catalytic activity in Na/O$_2$ cells.

Employing soluble catalysts (redox mediators) in the liquid electrolyte to facilitate the oxidation of Li$_2$O$_2$ upon charging has proved to be an effective way to improve the energy efficiency of Li/O$_2$ batteries.[71–73] Similar strategies were also conducted in Na/O$_2$ battery research. Yin et al. discovered that the addition
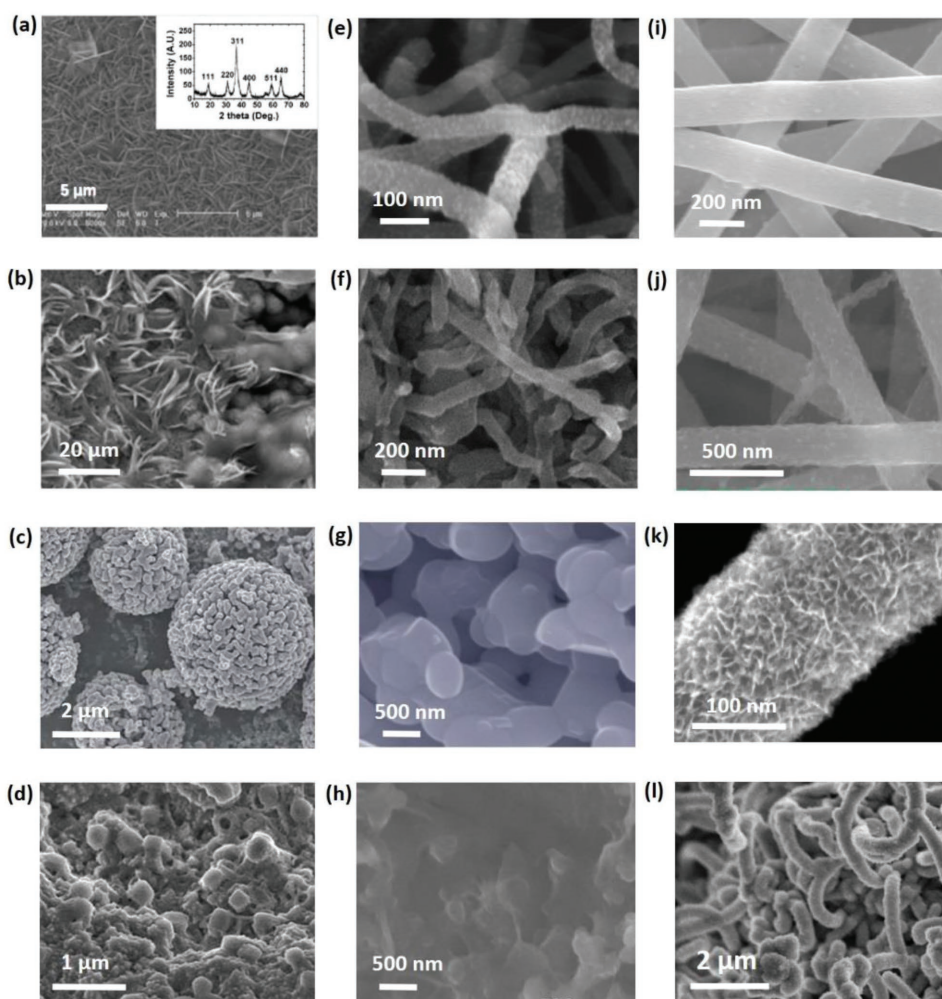

Figure 5. a) SEM image of NiCo$_2$O$_4$ nanosheets on Ni foam. Inset is the XRD pattern of the NiCo$_2$O$_4$ nanosheets. b) SEM image of a NiCo$_2$O$_4$ electrode discharged at a current density of 50 mA g^{-1}. a,b) Reproduced with permission.[36] Copyright 2014, Elsevier. SEM images of the synthesized c) CaMnO$_3$ and d) the CaMnO$_3$/C electrode after discharged to 2.0 V. c,d) Reproduced with permission.[37] Copyright 2015, The Royal Society of Chemistry. SEM images of e) the synthesized ALD CNT@Co$_3$O$_4$ and f) the ALD CNT@Co$_3$O$_4$ electrode after discharge at the current density of 150 mA g^{-1}. e,f) Reproduced with permission.[47] Copyright 2017, Wiley-VCH. SEM images of g) as-synthesized pyrochlore oxides La$_2$Co$_2$O$_7$ and h) discharged La$_2$Co$_2$O$_7$/SP electrode. g,h) Reproduced with permission.[55] Copyright 2017, The American Chemical Society. SEM images of i) as-prepared Co-ECNCFs and j) discharge products on Co-ECNCFs. i,j) Reproduced with permission.[57] Copyright 2017, Elsevier. SEM images of k) as-synthesized Gr/NCNT/MnO/Pd and l) the corresponding electrode discharged at a current density of 0.1 mA cm^{-2}. k,l) Reproduced with permission.[70] Copyright 2017, The Royal Society of Chemistry.

**ADVANCED
SCIENCE NEWS**
www.advancedsciencenews.com

**ADVANCED
MATERIALS
TECHNOLOGIES**
www.advmattechnol.de

of ferrocene or NaI as redox mediators in organic electrolytes could facilitate the decomposition of Na_2O_2 and reduce the charge overpotential of Na/O_2 batteries.[51,64] Later, they also observed that heterogeneous catalysts (Co_3O_4 nanowires) and a liquid redox mediator (ferrocene) showed a synergetic effect that could change the morphology of the discharge products from nanoflakes to nanofilms with significantly enhanced cycling performance.[40]

As one of the major discharge products, sodium superoxide (NaO_2) has been reported to be unstable in aprotic electrolytes and leads to the poor cycling stability of Na/O_2 cells. In contrast, the generation of sodium peroxide moieties ($Na_{2-x}O_2$ or their hydrates) may have an advantage in terms of better stability and higher energy density. Kang et al. used ruthenium decorated carbon nanotubes (CNT/Ru) as stationary catalysts to catalyze ORR and OER in Na/O_2 cells and successfully observed $Na_{2-x}O_2$ as the major discharge product.[74] Na/O_2 cells with CNT/Ru cathodes exhibited stable cycling performances over 100 cycles, which outperformed similar cells with CNT cathodes based on the formation and decomposition of NaO_2. Ma et al. also reported that Pd-decorated ZnO-coated graphitized carbon black (Pd/ZnO/C) promoted the formation/decomposition of Na_2O_2 during cell discharge/charge.[55] Meanwhile, the charge overpotential could be reduced to ≈0.5 V, which is much lower than those of previous reported Na_2O_2 based Na/O_2 cells.

The above reported outcomes indicate that employing carbon materials and other catalysts to optimize the porous structure and enhance the catalytic activities of the oxygen electrode can be a promising strategy to achieve high-performance rechargeable Na/O_2 batteries. The major challenge that needs to be resolved is to identify the controlling parameters for manipulating the morphologies and chemical compositions of discharge products.

4. Sodium Anodes

The use of a metal anode is motivated by the aim to maximize the practical energy density of Na/O_2 batteries. In the quest for high practical energy densities of alkali metal/oxygen cells, intensive research is needed to identify whether the metal anode can indeed be competitive.[9] It is reported that especially deep cycling with high charge/discharge capacities can lead to increased degradation of the alkali metal anode since the solid metal is depleted almost entirely in this case—an issue not only observed in alkali metal/oxygen cells but also in alkali metal/sulfur cells.[75–77] During charge, metal ions are often deposited at the electrode surface with a different morphology than initially present. This change in morphology leads by implication to an increase in surface area, which is then the origin for more extensive side reactions with the electrolyte. These side reactions lead, for example, to drying-out of the electrolyte in the battery during cycling.[75] Furthermore, oxygen that is dissolved in the liquid electrolyte can diffuse through the entire battery to the anode side and could react there with the pristine metal surface, forming insulating species, such as metal oxides, which increase the anode impedance. In addition to the increased ohmic resistance of the anode, this effect

would also imply a loss of the active material (sodium in this case). From a practical point of view, a loss of sodium might be compensated by using a larger metal anode than actually needed, decreasing the practical energy density of the cell.

4.1. Dendrite Formation

Dendrite formation is a complex phenomenon and various attempts have been made to describe and explain its origin, but no comprehensive answer has been found yet.[78] Dendrite formation in Na/O_2 cells has been investigated in a few studies. It is agreed that the growth of dendrites is inherently caused by the gradient of the electric potential between anode and cathode, as slight perturbations at the electrode surface lead to locally different electric fields. Often it is additionally reported to be linked to an inhomogenous distribution of current on the metal surface due to the fact that the solid electrolyte interphase (SEI) is not always formed in a homogeneous manner.[79,80] After many charge/discharge cycles, dendrite formation possess a severe risk for the operation of practical cells: Cell failure may occur due to short-circuiting of anode and cathode as soon as dendrites grow and penetrate the separator completely. Various countermeasures were proposed to minimize the extent of dendrite formation, although there is no ultimate countermeasure that guaranties the dendrite-free use of alkali metal electrodes in cells with liquid electrolytes up till now.[78,80]

Besides the loss of charge capacity and cell life time, the resulting formation of often flammable gases and, in particular, short-circuiting can result in serious safety issues. Many factors, which may influence dendrite growth have been discussed in the past, mainly originating from the general instability of planar surfaces (**Figure 6**), the inhomogeneous concentration profiles in the liquid electrolyte, and the composition of the SEI. The SEI might thereby stem from decomposition products from the reaction of liquid electrolyte with the metal anode. By choosing lower current densities, concentration inhomogeneities in the region of the electrode surface can be limited.[78] Suitable additives such as $NaPF_6$ in the electrolyte, which form electron blocking SEIs, have also been suggested.[81,82] Forming a SEI during battery set-up might be another option and recent studies have shown promising results thereof: Nazar et al. have evidenced the efficiency of a protective SEI in a lithium-based system.[77] Therein, they intentionally use an additive to create a protective SEI with a formation step during cycling, whereby they introduce the SEI as "alive" or formed in vivo. A tailor-made protective layer on the Na anode would certainly enhance the cycling stability and ensure safe operation of the metal electrodes from the practical point of view, however at the cost of slightly decreasing the specific energy due to additional weight of the protective layer.[17]

Very recently Medenbach et al. have presented a comprehensive study on the cause and effect of dendrites on Na/O_2 batteries.[78] By means of optical monitoring of the metal anode in a glass cell with an excess of electrolyte in combination with impedance spectroscopy, they gained fundamental insights into the morphological instabilities during discharge/charge and on the influence that a formed SEI has on dendrite formation. Thereafter, they designed practical studies for full cells, varying
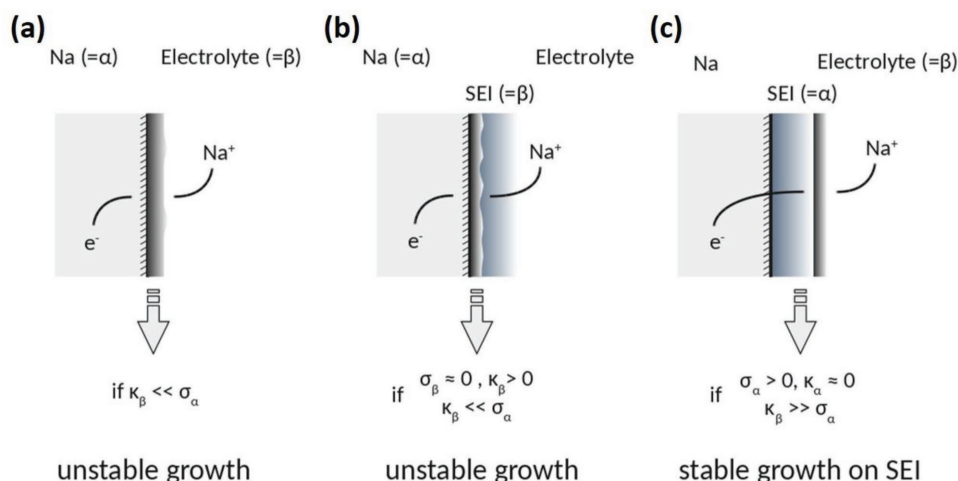
Figure 6. Different cases of growth of morphological instabilities (i.e., facilitating dendrite formation) at the phase boundary α/β, representing the anode of Na/O$_2$ cells. By implication, growth of pure Na metal through the solid electrolyte interphase (SEI) inevitably causes morphological instabilities, that is, nuclei for dendrites, which correlates well with experimentally observed behavior. Here, σ and κ are the conductivity for electrons and the conductivity for sodium ions, respectively. Reproduced with permission.[78] Copyright 2017, Wiley-VCH.

the separator thickness and type, the charge capacity limit, the current density profile, and using electrolyte additives such as NaF. The insights gained may propel the practical application of metal anodes in general.

4.2. Protected Anodes: The Need for Solid Electrolytes that Conduct Na$^+$

Adding a protective layer on top of the sodium metal is another strategy to mitigate dendrite formation and to achieve higher cycling stability. A protective layer can consist of a polymer, a polymer/solid electrolyte/polymer sandwich layer, or just a solid electrolyte (SE).[17,83,84] Contrary to the widespread opinion that a SE can prevent dendrite growth in total, it was impressively shown that enormous shear forces during the growth of Li can even break hard materials such as Li$_7$La$_3$Zr$_2$O$_{12}$ (LLZO), which will likely also be the case for Na.[85] Only a few systematic studies of the hardness of SEs have been conducted to date.[86]

Besides being mechanically stable, the SE should also be chemically stable in contact with Na. In the simplest case, the SE would be chemically stable, and therefore, the overall cell resistance remains constant during cycling. If the SE decomposes, either an ion conducting and electron blocking SEI, or an interphase with mixed ionic and electronic conductivity (MCI) is formed. In the first case, the SEI grows steadily, and therefore, cell resistances increase steadily as well. In the second case, the SE decomposes completely until the additional cell resistance due to the SE is eliminated and a short-circuit due to dendrite formation might occur. The quantitative analysis of the formed interphase is the focus of several studies.[87] Other critical parameters which should be known for the SE are the specific ionic conductivity σ and its activation energy E_A. Some superionic sodium SEs provide σ in the range of liquid electrolytes, which ensures sufficient ionic transfer at the interface between solid and liquid electrolyte.[88] Based on

these properties, we will present the most promising SEs and polymer electrolytes for Na/O$_2$ batteries in Section 5.2.

4.3. Other Approaches for Anodes

To further cope with the inherent issues at the anode side of cells, Bender et al. have recently replaced the sodium metal anode with presodiated carbon as anode, which yields capacities of $\approx$120 mA h g^{-1}. As a positive side effect, short-circuiting due to dendrites was found to be minimized when using this special type of anode.[12,89] Various groups have proposed easily processable and versatile alternatives, such as Na$_3$V$_2$(PO$_4$)$_3$ or a composite of Na and Na$_3$V$_2$(PO$_4$)$_3$.[90,91] Plating/striping cycling experiments of cells with these composite anodes extended the battery lifetime significantly in both ether- and carbonate-based electrolytes. Replacing sodium metal with a composite electrode or with a presodiated carbon electrode may also address the issue of side reactions with oxygen and moisture from the cathode side since they can act as protective layer, however, always at the penalty of additional weight, which in turn reduces the energy density of the respective battery.[89,92]

5. Electrolytes

The choice of a suitable electrolyte for room-temperature Na/O$_2$ batteries is a complex challenge because the electrolyte interacts with all three of the principal battery components—the anode, the separator, and the cathode. Beyond safety and environmental concerns, the electrolyte governs many intrinsic parameters, such as the ionic conductivity and the solubility of oxygen, contributing to the cycling performance of the Na/O$_2$ battery. Unfortunately, the development of suitable electrolytes has not been as intense as the research on new electrode materials, although the electrolyte functions in an essential role in Na/O$_2$ systems.[17]
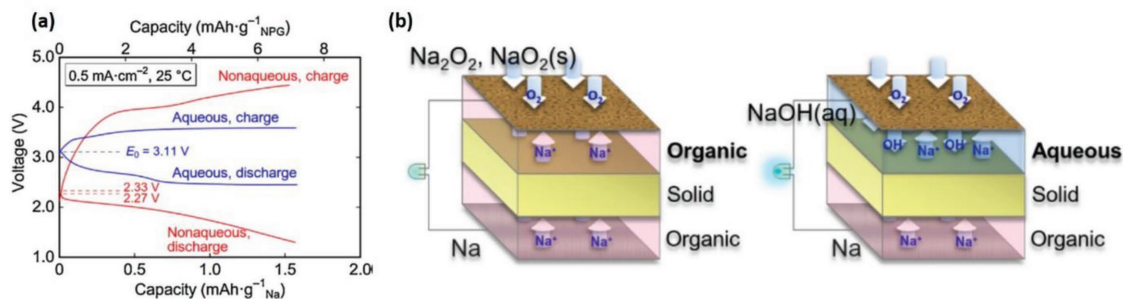
**ADVANCED
SCIENCE NEWS**
www.advancedsciencenews.com

**ADVANCED
MATERIALS
TECHNOLOGIES**
www.advmattechnol.de

Figure 7. a) First discharge and charge curves of Na/O$_2$ cells with aqueous and nonaqueous electrolytes (1 M NaOH used as aqueous electrolyte and EC:DMC 1:1 for organic electrolyte). b) Schematic configuration of nonaqueous (left) and aqueous (right) Na/O$_2$ cells. Reproduced with permission.[96] Copyright 2015, Elsevier.

5.1. Liquid Electrolytes

Within this subsection, we will solely focus on liquid electrolytes. The properties of a suitable liquid electrolyte for Na/O$_2$ batteries can be mainly delivered by its formulation from solvents and conducting salts. The salts should be highly soluble in the solvent to ensure sufficient conductivity of Na$^+$ between anode and cathode, and it needs to be stable during oxidation and reduction and also while interacting with the cell components.[54,93–95] It is reported that a suitable solvent must be polar, must possess a high dielectric constant, should exhibit a low viscosity, and ideally must not be involved in the battery reactions.[12,17,93–95] Overall, the electrolyte should show, among other minorly important properties, high ionic conductivity of $\approx$1–10 mS cm^{-1}, high solubility for oxygen, low volatility, low flammability, and a wide chemical and electrochemical stability window.[12,95] In this section we will give an overview of liquid electrolytes used in room-temperature rechargeable Na/O$_2$ batteries and the related challenges, as well as some strategies to overcome the limitations of electrolytes.

The first rechargeable Na/O$_2$ battery was fabricated by using molten sodium and a polymer electrolyte above 100 °C in 2011.[15] Since then fundamental research on Na/O$_2$ technology has progressed quickly, leading to the first room-temperature rechargeable Na/O$_2$ battery using nonaqueous electrolyte in 2012, and aqueous electrolyte on the cathode side of the cell in 2015.[15,16,93] Thereafter, a wide range of electrolytes have been tested in order to improve battery performance. Based on the electrolyte formulation and technical approaches, the electrolytes in room-temperature rechargeable Na/O$_2$ battery research can be divided into two main groups: aqueous electrolytes and nonaqueous electrolytes.

it should be kept in mind that aqueous Na/O$_2$ batteries do not require the use of an oxygen tank or supply of pure oxygen, which might decrease the weight and cost of the setup and might provide overall benefits for various technical reasons. Studies on Na/O$_2$ batteries with aqueous electrolytes prove that pore clogging of cathodes is prevented. Moreover, a low overpotential during charge can be maintained, while at the same time an increase in battery voltage of $E^0 = 3.11$ V (see **Figure 7**a) can be achieved. In addition, such cells are less sensitive to constituents from the surrounding air, and fast kinetics during ORR are observed.[14,96] Nonetheless, aqueous Na/O$_2$ batteries should be labeled as a hybrid nonaqueous/aqueous Na/O$_2$ batteries since a ceramic separator (NASICON) impregnated with organic solution (i.e., the anolyte) is used on top of the anode and aqueous electrolyte (i.e., the catholyte) is inserted between the separator and the cathode.[93,96,97] An overview and one example of the intriguing concept of a hybrid cell that utilizes anolyte and catholyte separated by a solid electrolyte is given elsewhere.[98,99] A recent impedance spectroscopy study reveals a remarkable difference between Na/O$_2$ batteries with aqueous and nonaqueous electrolytes (see Figure 7b for battery setup). Slower oxygen diffusion and reaction kinetics prevail in nonaqueous electrolyte compared to aqueous electrolytes.[96] So far, only NaOH alkaline aqueous electrolyte was used in room-temperature rechargeable Na/O$_2$ batteries; acidic electrolyte might not be used due to compatibility issues with the ceramic separator.[49,96,100] Although the use of aqueous electrolyte at the cathode can improve the Na/O$_2$ battery in many points, practical solutions to cope with the safety concerns associated with this type of configuration have to be developed—otherwise a leakage will lead to severe reactions of the Na metal at the anode with the aqueous solution at the cathode.

5.1.1. Aqueous Electrolytes

Although seeming counter-intuitive, using aqueous electrolyte in Na/O$_2$ batteries appears to be a promising strategy for addressing several problems occurring in nonaqueous Na/O$_2$ systems, such as formation of insoluble discharge products blocking oxygen access during discharge and leading to a poor cyclability, low power density, and high overpotential.[14] Adding further materials/components (such as anolytes and catholytes) may seem to be adding more weight and complexity. However,

5.1.2. Nonaqueous Electrolytes

In contrast, nonaqueous electrolytes are used for the majority of Na/O$_2$ batteries reported up until now. Applying these organic, nonaqueous electrolytes was an obvious choice in experimental studies on Na/O$_2$ batteries; they are also used in lithium-based batteries where their efficacy was clearly proven. Carbonate-based electrolytes, ether-based electrolytes and DMSO-based electrolytes with moderate concentrations of conducting salt are the most popular used electrolytes in room-temperature

**ADVANCED
SCIENCE NEWS**
www.advancedsciencenews.com

**ADVANCED
MATERIALS
TECHNOLOGIES**
www.advmattechnol.de

Table 2. Dielectric constant and viscosity of various solvents used in the Na/O_2 system. Reproduced with permission.[103] Copyright 2017, The Royal Society of Chemistry.

Solvent	Dielectric constant	Dynamic viscosity [mPa s]
Ethylene carbonate (EC)	89.6	1.90
Propylene carbonate (PC)	66.1	2.50
Dimethyl carbonate (DMC)	3.10	0.58
Diethyl carbonate (DEC)	2.82	0.75
Ethyl methyl carbonate (EMC)	2.40	0.65

rechargeable Na/O_2 batteries.[6,14,20,23,29,95,100] As for Li/O_2 batteries, organic electrolytes applied are well known to undergo decomposition at elevated cell potentials. More detailed studies are given elsewhere.[49,101] Room-temperature ionic liquids, such as 1-methyl-3-propylimidazolium bis(trifluoromethanesulfone) imide (PMIMTFSI) and N-methyl-N-propylpiperidinium bis(trifluoromethanesulfonyl) imide (PP13TFSI) were also tested. However, the stability of these electrolytes remains challenging when compared to other electrolytes.[20,100,102]

Ether-based electrolytes seem to be more stable against attack by superoxide intermediates and radicals, and possess a lower vapor pressure than carbonates-based electrolytes.[49] Moreover, ether-based electrolytes have been highly recommended when carbonaceous cathodes are used in Na/O_2 batteries.[49] However, the discharge products of ether-based electrolytes are highly dependent on the cell conditions and the oxygen atmosphere, i.e., on the humidity and other sources of protons used during charge and discharge.[23,26,44,49]

Possessing a high dielectric constant (compare **Table 2**), which increases the solubility of the salts, carbonate-based electrolytes have been chosen as good alternative.[103] Ethyl methyl carbonates (EMCs) possess a low viscosity, which favors the mobility of sodium ions. However, they also possess a low dielectric constant (see Table 2), which can be improved by choosing a suitable salt with low polarization such as NaPF$_6$ (see **Figure 8**), to gain high solubility and ionic mobility.[49,103] Recently, the utilization of additives, e.g., redox mediators, in room-temperature rechargeable Na/O_2 batteries was reported as a good strategy to enhance the battery performances.[51,64,104] In conclusion the optimization of electrolyte formulation for room-temperature Na/O_2 batteries is still at an early stage.

5.1.3. Highly Concentrated Electrolytes

Electrolyte degradation leads undeniably to a poor cycle life of Na/O_2 batteries and has driven many fundamental research studies on finding alternative electrolytes.[17] One possibility to mitigate electrolyte degradation might be the utilization of highly concentrated electrolytes. Increasing the salt concentration changes the solution chemistry and confers some advantages and disadvantages.[29,105] Superconcentrated electrolytes exhibit a very low volatility due to a limited amount of solvent molecules in the electrolyte, and thereby, have increased thermal stability, which leads to better battery performance and most importantly increased battery safety.[105] This concept is

not new and was successfully utilized in lithium-based batteries previously.[29,105] Since Na/O_2 battery systems are open to a gas phase at the cathode compartment, concentrated electrolytes should not be too volatile. On the other hand it is also necessary to promote the wetting of the cathode by the electrolyte.[106] Moreover, the effect of surrounding humidity or moisture is also drastically reduced (due to decreased solubility thereof) when the highly concentrated electrolyte is used. It is noteworthy that water has a big impact on the cell chemistry of the Na/O_2 system since water opens pathways to a multitude of side reactions with various short-lived oxygen species and thus reduces the reversibility of the battery.[18,26] Nevertheless, using concentrated electrolytes also brings many disadvantages, such as a low ion conductivity due to ion pairing, increase in viscosity of electrolyte, and slightly increased cost of the total materials.[105]

5.2. Solid Electrolytes

As mentioned in Section 4, protection of sodium anodes from a liquid electrolyte by applying a solid electrolyte (SE) is one concept to prevent cell degradation. In the following paragraphs, we comment on materials and material classes that are suitable to be used as SE and polymer electrolytes in Na/O_2 batteries.

5.2.1. Oxide Solid Electrolytes

The number of Na$^+$ conductors reported with sufficient ionic conductivity is low in comparison to the number of Li$^+$ conductors. Nevertheless, it was the β''-Al$_2$O$_3$ structure type, which originally prompted the term "super" ionic conductor.[107] A specific conductivity (σ) of 35 mS cm^{-1} was observed for single crystals of Mg-stabilized Na-β''-Al$_2$O$_3$. Measurements on polycrystalline samples reveal the typical drawback of these oxide compounds: Even highly compressed powders, which are annealed at high
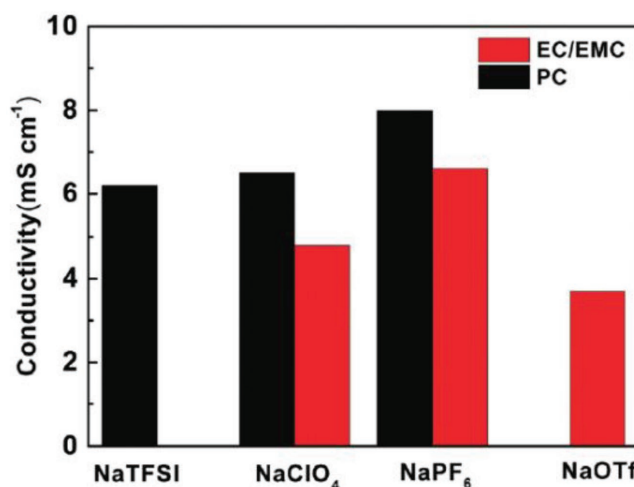

Figure 8. Conductivity of PC-based electrolyte with 1 M conducting salts (black) and EC/ECM (3.7 wt%)-based electrolyte with 0.8 M of conducting salts (red). Reproduced with permission.[103] Copyright 2017, The Royal Society of Chemistry.

temperatures above 1000 °C afterward, show a much lower conductivity of $\sigma = 7.8$ mS cm^{-1} compared to the single crystal value because additional resistances at the grain boundaries have to be taken into account. An activation energy E_A of 0.15 eV was estimated.[108] Increasing the phase stability even further with Li, the Li-stabilized Na-β''-Al$_2$O$_3$ attains 2.1 mS cm^{-1} and an E_A of 0.31 eV.[87] To improve the density and lower the resistance at the gain boundaries of polycrystalline samples, sol–gel synthesis is a suitable route. In combination with energy efficient microwave sintering, densities about 99% of theoretical can be reached.[109] Interestingly, methods such as slip casting, tape casting or electrophoretic deposition were shown to improve processing of thin SE membranes ($\approx$50 µm thick), which gives a promising outlook for future battery production.[110–112]

So far for Na anodes, Na-β''-Al$_2$O$_3$ is the only known SE, which has been proven to be stable against Na metal, wherefore it is preferably used in high-temperature Na/S or so-called ZEBRA (sodium/nickel chloride battery) batteries.[11] Their cell performance mainly suffers from the imperfect wetting of Na-β''-Al$_2$O$_3$ by molten sodium.[113–115] However, low cost precursors are available and make Na-β''-Al$_2$O$_3$ the best available sodium SE on the market to date. The closest competitor to Na-β''-Al$_2$O$_3$ is the NASICON structural type SE Na$_3$Zr$_2$Si$_2$PO$_{12}$, which shows a specific conductivity of 0.56 mS cm^{-1} paired with an activation energy of 0.37 eV.[116,117] A 10 wt% excess of the Na precursors can double σ by stabilizing the NASICON structure and minimizing the content of electrically insulating side phases such as ZrO$_2$. This also enables the use of slightly lower annealing temperatures of around 900 to 1100 °C.[118,119]

An intrinsic enhancement of the number of charge carriers and σ can be alternatively achieved by the substitution of Zr by subvalent cations.[120] Examples of well-performing bivalent-substituted NASICON SEs are Na$_{3.4}$Zr$_{1.8}$Zn$_{0.2}$Si$_2$PO$_{12}$ as well as Na$_{3.1}$Zr$_{1.95}$Mg$_{0.05}$Si$_2$PO$_{12}$ (about 3.5 mS cm^{-1}; activation energy of 0.32 eV).[121–123] They are only outperformed by Na$_{3.4}$Sc$_{0.4}$Zr$_{1.6}$Si$_2$PO$_{12}$, which shows a higher conductivity of 4.0 mS cm^{-1} and a lower activation energy of 0.26 eV.[124,125] Increasing the content of Na decreases the number of vacancies in the structure, which results in lower values of σ. Increasing the ratio of Si to P also enables a higher concentration of Na up to Na$_{3.4}$Sc$_2$Si$_{0.4}$P$_{2.2}$O$_{12}$, but lowers σ by one order of magnitude.[126,127]

Even though NASICON structures are chemically stable against air and moisture, samples should be stored and processed under Argon to prevent contact losses with the Na metal electrode, or at least heated to 600 °C before cell assembly.[128] In the case of high temperature applications, X-ray photoelectron spectroscopy (XPS) studies show that Zr, Si, and P get slightly reduced if directly in contact with Na metal.[129] An aqueous Na/O$_2$ battery in which Na was separated from a NaOH solution by a NASICON ceramic, exhibited an energy density of 1500 Wh kg^{-1} and a discharge capacity of 600 mA h g^{-1}. The main limiting factor is still the comparably high ohmic resistance of the ceramic separator.[130]

5.2.2. Thiophosphates

Inspired by the lithium thiophosphates Li$_{10}$GeP$_2$S$_{12}$ and Li$_{10}$SnP$_2$S$_{12}$, a stable phase Na$_{10}$SnP$_2$S$_{12}$ was predicted by ab

initio molecular dynamics (AIMD) simulations.[131–133] This sodium thiophosphate was also experimentally found to be a highly promising and stable superionic conductor. Interestingly, σ and E_A measured for Na$_{10}$Sn$_2$PS$_{12}$ differ in two recent studies: The reported values range between 1.4 and 3.7 S cm^{-1} and claimed activation energies vary between 0.25 and 0.39 eV, respectively.[134,135] Nonetheless, even if the lower Figure is chosen, this structure is the sodium thiophosphate with the highest reported specific ionic conductivity for Na$^+$ so far. However, since Li$_{10}$SnP$_2$S$_{12}$ is found to be thermodynamically unstable against Li, the use of Na$_{10}$Sn$_2$PS$_{12}$ in direct contact with Na may prove problematic. Thiophosphates with the composition Na$_3$AS$_4$ (A = P, As, Sb) provide comparably low specific ionic conductivities in the range between 0.1 and 0.001 mS cm^{-1}.[136] Thereby, a 3D pathway for Na transport is proposed.[136,137]

A Na-Sn/Na$_3$PS$_4$/TiS$_2$ battery with a cell voltage of 1.6 V showed a capacity of 90 mA h g^{-1} for 10 cycles, which can be seen as highly promising for Na/O$_2$ batteries as well.[138] In addition to the lower value of σ, Na$_3$PS$_4$ has another disadvantage in comparison to the above-mentioned oxide ceramics. It decomposes in contact with Na metal and forms an interphase, which consists of ion blocking Na$_2$S and Na$_3$P. This causes an increase of the cell resistance.[87] It is also extremely prone to side reactions with components of air, in particular moisture.[136,139]

In conclusion, the group of oxide ceramics with Na-β''-Al$_2$O$_3$ and NASICON structure can be seen as most promising SEs for practical uses in Na/O$_2$ batteries. They exhibit sufficient ionic conductivity for sodium ions (compare **Table 3**), are stable against humidity and other components of air, and are highly stable against metallic sodium. One drawback is the reduced ionic conductivity due to grain boundaries formed in the processed samples compared to single crystals of the respective structures and the possibly cost-intensive synthesis at elevated temperatures (apart from sol–gel methods). Challenges with processing and cost of SEs will possibly remain for the successful implementation of Na/O$_2$ batteries with an anode that is protected by a SE in practical applications.

5.2.3. Solid Polymer Electrolyte

Solid polymer electrolytes (SPE) belong to another class of materials that can be applied as a separator in metal/oxygen

Table 3. Summary of properties for the most promising solid electrolytes for the application in sodium oxygen batteries presented in Section 5.3.

Compound	σ [mS cm^{-1}]	E_A [eV]	Reference
Na$_{1.7}$Li$_{0.3}$Al$_{10.7}$O$_{17}$	2.1	0.31	[87]
(Na$_2$O)$_{12}$(MgO)$_5$(Al$_2$O$_3$)$_{83}$	7.8	0.15	[109]
Na$_3$Zr$_2$Si$_2$PO$_{12}$	0.56	0.37	[118]
Na$_{3.1}$Zr$_{1.95}$Mg$_{0.05}$Si$_2$PO$_{12}$	3.5	0.32	[123]
Na$_{3.4}$Sc$_{0.4}$Zr$_{1.6}$ Si$_2$PO$_{12}$	4	0.26	[125]
Na$_{10}$Sn$_2$PS$_{12}$	3.7	0.38	[136]
Na$_3$PS$_4$ (glass ceramic)	0.2	0.28	[139]

**ADVANCED
SCIENCE NEWS**
www.advancedsciencenews.com

**ADVANCED
MATERIALS
TECHNOLOGIES**
www.advmattechnol.de

batteries because SPEs are mechanically flexible and generally adhere better to both the anode or the cathode in comparison to SEs.[140] The first solid polymer electrolyte used for Na/O$_2$ batteries was based on polyethylene glycol dimethyl ether operating at 100 °C.[15] SPEs are still relatively unexplored in the field of Na/O$_2$ batteries or even Na-ion batteries, which might be due to many encountered challenges, such as poor ionic conductivity and limited stability.[94,103,141] However, SPEs are widely applied in lithium-based batteries. On this basis, we will discuss possible SPEs for Na/O$_2$ batteries and briefly derive the requirements that they should meet to be applicable.

SPEs are typically poor solvents for ions, and thus, have poor ionic conductivity at room-temperature, and better ionic conductivity of around 1.0 mS cm^{-1} at high temperature (e.g., NaTFSI-polyethylene oxide at 70 °C).[94] SPEs used either in Na-ion batteries and/or in Li/O$_2$ batteries could be good candidates for Na/O$_2$ batteries as well, since the battery systems share some similarities: In Li/O$_2$ batteries, SPEs were successfully applied for example using polyacrylonitrile (PAN)-based or polyethylene oxide (PEO)-based polymer electrolytes.[142–145] It should be noted that most batteries with SPEs need to operate at even higher temperatures (up to 120 °C) to ensure good ionic conductivity and battery performance. Similarly, some polymer electrolytes were successfully applied in Na-ion batteries: In general, PEO-based electrolytes with NaClO$_4$ as conducting salt (σ of 3.1×10^{-3} mS cm^{-1} at 60 °C), PEO-NaPF$_6$ (σ of 5.0×10^{-3} mS cm^{-1} at room-temperature) or PEO-NaClO$_3$ (σ of 1.0×10^{-5} mS at room-temperature).[146–148] Alternative polymer materials are based on poly(vinyl alcohol) (PVA) or poly(vinyl pyrrolidone) (PVP) with several conductive salts, such as NaF, NaBr, NaClO$_3$, or NaClO$_4$.[149–151] It should be noted that all SPEs may contain residues of water in the polymer backbone due to their synthesis route. Residues of water might react directly with the Na metal surface, diminishing anode stability and performance. However, SPEs possess ionic conductivity at room-temperature which require optimization before they might be applied in Na/O$_2$ batteries.

6. Outlook and Future Perspectives

Regarding energy density and cost, the rechargeable Na/O$_2$ battery technology attracts increasing attention because it might be able to amend the market for portable and large-scale energy storage. However, in view of a practical energy storage device that might replace lithium-ion batteries, the Na/O$_2$ battery is still in its infant stage. Although significant progress has been achieved—as we presented in this review—several critical issues need to be resolved before practical applications can be achieved. From cell design to each cell component, research outcomes regarding to the essential factors that have a significant influence on the electrochemical performance of Na/O$_2$ cells have been discussed, including the reaction mechanism underpinning the complex chemical/electrochemical reactions, the design of porous oxygen electrodes with appropriate catalysts, the stability of the Na metal anode and electrolytes.

Porous oxygen electrodes play an essential role to achieve high-performance Na/O$_2$ cells. Intensive research activities were devoted to investigating how cathode materials affect the formation of discharge products, i.e., NaO$_2$ or Na$_2$O$_2$, energy density, cycling efficiency, and power density of Na/O$_2$ cells. Carbon-based materials are the best choice for oxygen electrode at the current stage. However, the formation and growth mechanisms of different discharge products on the cathodes is still debated. To develop high efficiency and stable oxygen electrodes, this matter needs to be further clarified through a variety of in situ and ex situ characterization methods.

In parallel with the importance of the cathode, electrolytes function in an essential role to determine whether a Na/O$_2$ cell can be truly rechargeable. Currently, one of the major challenges for the development of long service life Na/O$_2$ cells is the search for stable electrolytes. Ether-based electrolytes are widely used due to their relative stability against reduced oxygen species for both Li/O$_2$ and Na/O$_2$ cells.[59] However, their stability during long-term cycling remains unclear. In addition, as an indispensable component of the electrolytes, sodium salt, deserves more attention since it can improve the stability of electrolytes against other cell components and discharge products in Na/O$_2$ cells. Undoubtedly, identifying a completely stable electrolyte to tolerate the highly oxidizing environment in the presence of oxygen during cycling must be a research priority. Designing an efficient method to identify the stability of electrolytes is a great challenge but would be beneficial to develop practical Na/O$_2$ batteries.

Developing a stable Na metal anode is an unavoidable challenge for achieving Na metal-based battery systems with long-service life.[81] To protect the Na anode from oxygen and moisture crossover from the oxygen electrode, in situ formation of passivating films on Na metal anodes though reactions between electrolyte and Na metal or applying artificial protecting layers on Na metal anodes will be crucial for the development of high performance Na/O$_2$ cells. These protective layers must meet the following criteria: 1) They need to have high ionic conductivity to facilitate easy and uniform transport of Na-ions throughout the entire electrode surface. 2) They need to be homogeneous in all aspects to facilitate Na metal nucleation and growth. 3) They must possess a high enough elastic modulus and compact structure to suppress dendrite formation. 4) They have to be flexible enough to accommodate interface fluctuation during Na plating/striping. 5) They should block oxygen and moisture crossover from the oxygen electrode to the Na anode. The development of advanced technologies is anticipated to fabricate nanoscale thin films as protective layers to meet the above-mentioned criteria.

In conclusion, even in their infant stage of research, Na/O$_2$ cells show attractive properties and recent research activities in this new field have gained momentum. However, rechargeable Na/O$_2$ batteries are still far from being practical and applicable in any real device or application. Significant progress related to cell reaction mechanisms, cell configuration design, and cell components must be achieved before this new concept can be utilized. Therefore, innovations in fundamental research, materials design, and technical development are urgently required.

[1] G. P. Peters, R. M. Andrew, T. Boden, J. G. Canadell, P. Ciais, C. Le Quere, G. Marland, M. R. Raupach, C. Wilson, *Nat. Clim. Change* **2013**, *3*, 4.

[2] J. Lu, L. Li, J.-B. Park, Y.-K. Sun, F. Wu, K. Amine, *Chem. Rev.* **2014**, *114*, 5611.

[3] P. G. Bruce, S. A. Freunberger, L. J. Hardwick, J. M. Tarascon, *Nat. Mater.* **2012**, *11*, 19.

[4] A. Philipp, *Angew. Chem., Int. Ed.* **2018**, *57*, 6710.

[5] G. Girishkumar, B. McCloskey, A. C. Luntz, S. Swanson, W. Wilcke, *J. Phys. Chem. Lett.* **2010**, *1*, 2193.

[6] K. Song, D. A. Agyeman, M. Park, J. Yang, Y.-M. Kang, *Adv. Mater.* **2017**, *29*, 1606572.

[7] M. M. O. Thotiyl, S. A. Freunberger, Z. Peng, P. G. Bruce, *J. Am. Chem. Soc.* **2013**, *135*, 494.

[8] Z. L. Wang, D. Xu, J. J. Xu, X. B. Zhang, *Chem. Soc. Rev.* **2014**, *43*, 7746.

[9] K. G. Gallagher, S. Goebel, T. Greszler, M. Mathias, W. Oelerich, D. Eroglu, V. Srinivasan, *Energy Environ. Sci.* **2014**, *7*, 1555.

[10] M. D. Slater, D. Kim, E. Lee, C. S. Johnson, *Adv. Funct. Mater.* **2013**, *23*, 947.

[11] P. Hartmann, C. L. Bender, M. Vracar, A. K. Duerr, A. Garsuch, J. Janek, P. Adelhelm, *Nat. Mater.* **2013**, *12*, 228.

[12] I. Landa-Medrano, C. Li, N. Ortiz-Vitoriano, I. Ruiz de Larramendi, J. Carrasco, T. Rojo, *J. Phys. Chem. Lett.* **2016**, *7*, 1161.

[13] E. Peled, D. Golodnitsky, R. Hadar, H. Mazor, M. Goor, L. Burstein, *J. Power Sources* **2013**, *244*, 771.

[14] S. K. Das, S. Lau, L. A. Archer, *J. Mater. Chem. A* **2014**, *2*, 12623.

[15] E. Peled, D. Golodnitsky, H. Mazor, M. Goor, S. Avshalomov, *J. Power Sources* **2011**, *196*, 6835.

[16] Q. Sun, Y. Yang, Z.-W. Fu, *Electrochem. Commun.* **2012**, *16*, 22.

[17] H. Yadegari, Q. Sun, X. Sun, *Adv. Mater.* **2016**, *28*, 7065.

[18] C. L. Bender, D. Schröder, R. Pinedo, P. Adelhelm, J. Janek, *Angew. Chem., Int. Ed.* **2016**, *55*, 4640.

[19] S. Ma, W. C. McKee, J. Wang, L. Guo, M. Jansen, Y. Xu, Z. Peng, *Phys. Chem. Chem. Phys.* **2017**, *19*, 12375.

[20] I. M. Aldous, L. J. Hardwick, *Angew. Chem., Int. Ed.* **2016**, *55*, 8254.

[21] N. Zhao, C. Li, X. Guo, *Phys. Chem. Chem. Phys.* **2014**, *16*, 15646.

[22] C. L. Bender, P. Hartmann, M. Vracar, P. Adelhelm, J. Janek, *Adv. Energy Mater.* **2014**, *4*, 1301863.

[23] B. D. McCloskey, J. M. Garcia, A. C. Luntz, *J. Phys. Chem. Lett.* **2014**, *5*, 1230.

[24] N. Ortiz-Vitoriano, T. P. Batcho, D. G. Kwabi, B. Han, N. Pour, K. P. C. Yao, C. V. Thompson, Y. Shao-Horn, *J. Phys. Chem. Lett.* **2015**, *6*, 2636.

[25] I. I. Abate, L. E. Thompson, H.-C. Kim, N. B. Aetukuri, *J. Phys. Chem. Lett.* **2016**, *7*, 2164.

[26] C. Xia, R. Black, R. Fernandes, B. Adams, L. F. Nazar, *Nat. Chem.* **2015**, *7*, 496.

[27] P. Hartmann, C. L. Bender, J. Sann, A. K. Duerr, M. Jansen, J. Janek, P. Adelhelm, *Phys. Chem. Chem. Phys.* **2013**, *15*, 11661.

[28] X. Bi, X. Ren, Z. Huang, M. Yu, E. Kreidler, Y. Wu, *Chem. Commun.* **2015**, *51*, 7665.

[29] M. He, K. C. Lau, X. Ren, N. Xiao, W. D. McCulloch, L. A. Curtiss, Y. Wu, *Angew. Chem., Int. Ed.* **2016**, *128*, 15536.

[30] J. Kim, H. Park, B. Lee, W. M. Seong, H.-D. Lim, Y. Bae, H. Kim, W. K. Kim, K. H. Ryu, K. Kang, *Nat. Commun.* **2016**, *7*, 10670.

[31] T. Liu, G. Kim, M. T. L. Casford, C. P. Grey, *J. Phys. Chem. Lett.* **2016**, *7*, 4841.

[32] L. Lutz, W. Yin, A. Grimaud, D. Alves Dalla Corte, M. Tang, L. Johnson, E. Azaceta, V. Sarou-Kanian, A. J. Naylor, S. Hamad, J. A. Anta, E. Salager, R. Tena-Zaera, P. G. Bruce, J. M. Tarascon, *J. Phys. Chem. C* **2016**, *120*, 20068.

[33] C. Liu, D. Rehnlund, W. R. Brant, J. Zhu, T. Gustafsson, R. Younesi, *ACS Energy Lett.* **2017**, *2*, 2440.

[34] L. Lutz, D. Alves Dalla Corte, M. Tang, E. Salager, M. Deschamps, A. Grimaud, L. Johnson, P. G. Bruce, J.-M. Tarascon, *Chem. Mater.* **2017**, *29*, 6066.

[35] Y. Li, H. Yadegari, X. Li, M. N. Banis, R. Li, X. Sun, *Chem. Commun.* **2013**, *49*, 11731.

[36] W.-M. Liu, W.-W. Yin, F. Ding, L. Sang, Z.-W. Fu, *Electrochem. Commun.* **2014**, *45*, 87.

[37] Y. Hu, X. Han, Q. Zhao, J. Du, F. Cheng, J. Chen, *J. Mater. Chem. A* **2015**, *3*, 3320.

[38] W. Liu, Q. Sun, Y. Yang, J.-Y. Xie, Z.-W. Fu, *Chem. Commun.* **2013**, *49*, 1951.

[39] H. Yadegari, M. N. Banis, B. Xiao, Q. Sun, X. Li, A. Lushington, B. Wang, R. Li, T.-K. Sham, X. Cui, X. Sun, *Chem. Mater.* **2015**, *27*, 3040.

[40] W.-W. Yin, Z.-W. Fu, *Chem. Commun.* **2017**, *53*, 1522.

[41] Q. Sun, H. Yadegari, M. N. Banis, J. Liu, B. Xiao, B. Wang, S. Lawes, X. Li, R. Li, X. Sun, *Nano Energy* **2015**, *12*, 698.

[42] S. Kang, Y. Mo, S. P. Ong, G. Ceder, *Nano Lett.* **2014**, *14*, 1016.

[43] H. Yadegari, Y. Li, M. N. Banis, X. Li, B. Wang, Q. Sun, R. Li, T.-K. Sham, X. Cui, X. Sun, *Energy Environ. Sci.* **2014**, *7*, 3747.

[44] X. Bi, R. Wang, L. Ma, D. Zhang, K. Amine, J. Lu, *Small Methods* **2017**, *1*, 1700102.

[45] B. Sun, K. Kretschmer, X. Xie, P. Munroe, Z. Peng, G. Wang, *Adv. Mater.* **2017**, *29*, 1606816.

[46] L. Ma, D. Zhang, Y. Lei, Y. Yuan, T. Wu, J. Lu, K. Amine, *ACS Energy Lett.* **2018**, *3*, 276.

[47] Q. Sun, J. Liu, X. Li, B. Wang, H. Yadegari, A. Lushington, M. N. Banis, Y. Zhao, W. Xiao, N. Chen, J. Wang, T.-K. Sham, X. Sun, *Adv. Funct. Mater.* **2017**, *27*, 1606662.

[48] C. L. Bender, W. Bartuli, M. G. Schwab, P. Adelhelm, J. Janek, *Energy Technol.* **2015**, *3*, 242.

[49] R. Black, A. Shyamsunder, P. Adeli, D. Kundu, G. K. Murphy, L. F. Nazar, *ChemSusChem* **2016**, *9*, 1795.

[50] S. Zhang, Z. Wen, J. Jin, T. Zhang, J. Yang, C. Chen, *J. Mater. Chem. A* **2016**, *4*, 7238.

[51] W.-W. Yin, Z. Shadike, Y. Yang, F. Ding, L. Sang, H. Li, Z.-W. Fu, *Chem. Commun.* **2015**, *51*, 2324.

[52] Z. Jian, Y. Chen, F. Li, T. Zhang, C. Liu, H. Zhou, *J. Power Sources* **2014**, *251*, 466.

[53] J. Kim, H.-D. Lim, H. Gwon, K. Kang, *Phys. Chem. Chem. Phys.* **2013**, *15*, 3623.

[54] J.-l. Ma, X.-b. Zhang, *J. Mater. Chem. A* **2016**, *4*, 10008.

[55] N. Li, Y. Yin, F. Meng, Q. Zhang, J. Yan, Q. Jiang, *ACS Catal.* **2017**, *7*, 7688.

[56] C. Shu, Y. Lin, B. Zhang, S. B. A. Hamid, D. Su, *J. Mater. Chem. A* **2016**, *4*, 6610.

[57] J.-L. Ma, F.-L. Meng, D. Xu, X.-B. Zhang, *Energy Storage Mater.* **2017**, *6*, 1.

[58] S. H. Oh, R. Black, E. Pomerantseva, J.-H. Lee, L. F. Nazar, *Nat. Chem.* **2012**, *4*, 1004.

[59] H.-G. Jung, J. Hassoun, J.-B. Park, Y.-K. Sun, B. Scrosati, *Nat. Chem.* **2012**, *4*, 579.

[60] D. Schröder, C. L. Bender, M. Osenberg, A. Hilger, I. Manke, J. Janek, *Sci. Rep.* **2016**, *6*, 24288.

[61] J. Xiao, D. H. Mei, X. L. Li, W. Xu, D. Y. Wang, G. L. Graff, W. D. Bennett, Z. M. Nie, L. V. Saraf, I. A. Aksay, J. Liu, J. G. Zhang, *Nano Lett.* **2011**, *11*, 5071.

[62] B. Sun, B. Wang, D. W. Su, L. D. Xiao, H. Ahn, G. X. Wang, *Carbon* **2012**, *50*, 727.

[63] S. Kumar, B. Kishore, N. Munichandraiah, *RSC Adv.* **2016**, *6*, 63477.

[64] W.-W. Yin, J.-L. Yue, M.-H. Cao, W. Liu, J.-J. Ding, F. Ding, L. Sang, Z.-W. Fu, *J. Mater. Chem. A* **2015**, *3*, 19027.

[65] Y.-C. Lu, Z. Xu, H. A. Gasteiger, S. Chen, K. Hamad-Schifferli, Y. Shao-Horn, *J. Am. Chem. Soc.* **2010**, *132*, 12170.

[66] J.-J. Xu, Z.-L. Wang, D. Xu, L.-L. Zhang, X.-B. Zhang, *Nat. Commun.* **2013**, *4*, 2438.

[67] B. Sun, P. Munroe, G. Wang, *Sci. Rep.* **2013**, *3*, 2247.

[68] B. Sun, X. Huang, S. Chen, P. Munroe, G. Wang, *Nano Lett.* **2014**, *14*, 3145.

[69] S. Zhang, Z. Wen, K. Rui, C. Shen, Y. Lu, J. Yang, *J. Mater. Chem. A* **2015**, *3*, 2568.

[70] H. Yadegari, M. N. Banis, A. Lushington, Q. Sun, R. Li, T.-K. Sham, X. Sun, *Energy Environ. Sci.* **2017**, *10*, 286.

[71] Y. Chen, S. A. Freunberger, Z. Peng, O. Fontaine, P. G. Bruce, *Nat. Chem.* **2013**, *5*, 489.

[72] T. Liu, M. Leskes, W. Yu, A. J. Moore, L. Zhou, P. M. Bayley, G. Kim, C. P. Grey, *Science* **2015**, *350*, 530.

[73] J. B. Park, S. H. Lee, H. G. Jung, D. Aurbach, Y. K. Sun, *Adv. Mater.* **2018**, *30*, 1704162.

[74] J.-H. Kang, W.-J. Kwak, D. Aurbach, Y.-K. Sun, *J. Mater. Chem. A* **2017**, *5*, 20678.

[75] R. Fang, S. Zhao, Z. Sun, D. W. Wang, H. M. Cheng, F. Li, *Adv. Mater.* **2017**, *48*, 1606823.

[76] Y. Liu, Y. Cui, *Joule* **2017**, *1*, 649.

[77] Q. Pang, X. Liang, A. Shyamsunder, L. F. Nazar, *Joule* **2017**, *1*, 871.

[78] L. Medenbach, C. L. Bender, R. Haas, B. Mogwitz, C. Pompe, P. Adelhelm, D. Schröder, J. Janek, *Energy Technol.* **2017**, *5*, 2265.

[79] M. D. Pritzker, T. Z. Fahidy, *Electrochim. Acta* **1992**, *37*, 103.

[80] H. Kim, G. Jeong, Y.-U. Kim, J.-H. Kim, C.-M. Park, H.-J. Sohn, *Chem. Soc. Rev.* **2013**, *42*, 9011.

[81] Z. W. Seh, J. Sun, Y. Sun, Y. Cui, *ACS Cent. Sci.* **2015**, *1*, 449.

[82] S. Wu, Y. Qiao, K. Jiang, Y. He, S. Guo, H. Zhou, *Adv. Funct. Mater.* **2018**, *28*, 1706374.

[83] K. Liu, A. Pei, H. R. Lee, B. Kong, N. Liu, D. Lin, Y. Liu, C. Liu, P.-c. Hsu, Z. Bao, Y. Cui, *J. Am. Chem. Soc.* **2017**, *139*, 4815.

[84] W. Zhou, S. Wang, Y. Li, S. Xin, A. Manthiram, J. B. Goodenough, *J. Am. Chem. Soc.* **2016**, *138*, 9385.

[85] L. Porz, T. Swamy, B. W. Sheldon, D. Rettenwander, T. Frömling, H. L. Thaman, S. Berendts, R. Uecker, W. C. Carter, Y.-M. Chiang, *Adv. Energy Mater.* **2017**, *7*, 1701003.

[86] F. P. McGrogan, T. Swamy, S. R. Bishop, E. Eggleton, L. Porz, X. Chen, Y. M. Chiang, K. J. Van Vliet, *Adv. Energy Mater.* **2017**, *7*, 1602011.

[87] S. Wenzel, T. Leichtweiss, D. A. Weber, J. Sann, W. G. Zeier, J. r. Janek, *ACS Appl. Mater. Interfaces* **2016**, *8*, 28216.

[88] F. Sagane, T. Abe, Z. Ogumi, *J. Power Sources* **2010**, *195*, 7466.

[89] C. L. Bender, B. Jache, P. Adelhelm, J. Janek, *J. Mater. Chem. A* **2015**, *3*, 20633.

[90] A. Wang, X. Hu, H. Tang, C. Zhang, S. Liu, Y. Yang, Q. Yang, J. Luo, *Angew. Chem., Int. Ed.* **2017**, *56*, 11921.

[91] Y. Zhang, L. Ma, L. Zhang, Z. Peng, *J. Electrochem. Soc.* **2016**, *163*, A1270.

[92] D. Schröder, C. L. Bender, R. Pinedo, W. Bartuli, M. G. Schwab, Ž. Tomovi , J. Janek, *Energy Technol.* **2017**, *5*, 1242.

[93] S. H. Sahgong, S. Senthilkumar, K. Kim, S. M. Hwang, Y. Kim, *Electrochem. Commun.* **2015**, *61*, 53.

[94] A. Ponrouch, D. Monti, A. Boschin, B. Steen, P. Johansson, M. Palacin, *J. Mater. Chem. A* **2015**, *3*, 22.

[95] X. Zhang, X.-G. Wang, Z. Xie, Z. Zhou, *Green Energy Environ.* **2016**, *1*, 4.

[96] T. Hashimoto, K. Hayashi, *Electrochim. Acta* **2015**, *182*, 809.

[97] W.-W. Yin, Z.-W. Fu, *ChemCatChem* **2017**, *9*, 1545.

[98] M. Arumugam, L. Longjun, *Adv. Energy Mater.* **2015**, *5*, 1401302.

[99] B. J. Bergner, M. R. Busche, R. Pinedo, B. B. Berkes, D. Schröder, J. Janek, *ACS Appl. Mater. Interfaces* **2016**, *8*, 7756.

[100] N. Zhao, X. Guo, *J. Phys. Chem. C* **2015**, *119*, 25319.

[101] D. Sharon, M. Afri, M. Noked, A. Garsuch, A. A. Frimer, D. Aurbach, *J. Phys. Chem. Lett.* **2013**, *4*, 3115.

[102] M. Kar, T. J. Simons, M. Forsyth, D. R. MacFarlane, *Phys. Chem. Chem. Phys.* **2014**, *16*, 18658.

[103] H. Che, S. Chen, Y. Xie, H. Wang, K. Amine, X.-Z. Liao, Z.-F. Ma, *Energy Environ. Sci.* **2017**, *10*, 1075.

[104] J. T. Frith, I. Landa-Medrano, I. Ruiz de Larramendi, T. Rojo, J. R. Owen, N. Garcia-Araez, *Chem. Commun.* **2017**, *53*, 12008.

[105] Y. Yamada, A. Yamada, *J. Electrochem. Soc.* **2015**, *162*, A2406.

[106] L. Suo, O. Borodin, T. Gao, M. Olguin, J. Ho, X. Fan, C. Luo, C. Wang, K. Xu, *Science* **2015**, *350*, 938.

[107] W. Roth, *J. Solid State Chem.* **1972**, *4*, 60.

[108] A. Hooper, *J. Phys. D: Appl. Phys.* **1977**, *10*, 1487.

[109] J. Wang, X.-P. Jiang, X.-L. Wei, H. Yang, X.-D. Shen, *J. Alloys Compd.* **2010**, *497*, 295.

[110] A. Mali, A. Petric, *J. Power Sources* **2011**, *196*, 5191.

[111] J. Y. Kim, N. L. Canfield, J. F. Bonnett, V. L. Sprenkle, K. Jung, I. Hong, *Solid State Ionics* **2015**, *278*, 192.

[112] X.-l. Wei, Y. Xia, X.-m. Liu, H. Yang, X.-d. Shen, *Electrochim. Acta* **2014**, *136*, 250.

[113] X. Lu, G. Li, J. Y. Kim, D. Mei, J. P. Lemmon, V. L. Sprenkle, J. Liu, *Nat. Commun.* **2014**, *5*, 4578.

[114] I. Kim, J.-Y. Park, C. H. Kim, J.-W. Park, J.-P. Ahn, J.-H. Ahn, K.-W. Kim, H.-J. Ahn, *J. Power Sources* **2016**, *301*, 332.

[115] G. Li, X. Lu, J. Y. Kim, J. P. Lemmon, V. L. Sprenkle, *J. Power Sources* **2014**, *249*, 414.

[116] J. Goodenough, H.-P. Hong, J. Kafalas, *Mater. Res. Bull.* **1976**, *11*, 203.

[117] W. Baur, J. Dygas, D. Whitmore, J. Faber, *Solid State Ionics* **1986**, *18*, 935.

[118] N. S. Bell, C. Edney, J. S. Wheeler, D. Ingersoll, E. D. Spoerke, *J. Am. Ceram. Soc.* **2014**, *97*, 3744.

[119] H. Park, K. Jung, M. Nezafati, C.-S. Kim, B. Kang, *ACS Appl. Mater. Interfaces* **2016**, *8*, 27814.

[120] A. G. Jolley, D. D. Taylor, N. J. Schreiber, E. D. Wachsman, *J. Am. Ceram. Soc.* **2015**, *98*, 2902.

[121] A. G. Jolley, G. Cohn, G. T. Hitz, E. D. Wachsman, *Ionics* **2015**, *21*, 3031.

[122] S. Song, H. M. Duong, A. M. Korsunsky, N. Hu, L. Lu, *Sci. Rep.* **2016**, *6*, 32330.

[123] M. Samiee, B. Radhakrishnan, Z. Rice, Z. Deng, Y. S. Meng, S. P. Ong, J. Luo, *J. Power Sources* **2017**, *347*, 229.

[124] Q. Ma, M. Guin, S. Naqash, C.-L. Tsai, F. Tietz, O. Guillon, *Chem. Mater.* **2016**, *28*, 4821.

[125] M. Kaus, M. Guin, M. Yavuz, M. Knapp, F. Tietz, O. Guillon, H. Ehrenberg, S. Indris, *J. Phys. Chem. C* **2017**, *121*, 1449.

[126] M. Guin, F. Tietz, O. Guillon, *Solid State Ionics* **2016**, *293*, 18.

[127] M. Guin, E. Dashjav, C. Kumar, F. Tietz, O. Guillon, *Solid State Sci.* **2017**, *67*, 30.

[128] M. Guin, S. Indris, M. Kaus, H. Ehrenberg, F. Tietz, O. Guillon, *Solid State Ionics* **2017**, *302*, 102.

[129] W. Zhou, Y. Li, S. Xin, J. B. Goodenough, *ACS Cent. Sci.* **2017**, *3*, 52.

[130] K. Hayashi, K. Shima, F. Sugiyama, *J. Electrochem. Soc.* **2013**, *160*, A1467.

[131] N. Kamaya, K. Homma, Y. Yamakawa, M. Hirayama, R. Kanno, M. Yonemura, T. Kamiyama, Y. Kato, S. Hama, K. Kawamoto, *Nat. Mater.* **2011**, *10*, 682.

[132] P. Bron, S. Johansson, K. Zick, J. r. Schmedt auf der Günne, S. Dehnen, B. Roling, *J. Am. Chem. Soc.* **2013**, *135*, 15694.

[133] W. D. Richards, T. Tsujimura, L. J. Miara, Y. Wang, J. C. Kim, S. P. Ong, I. Uechi, N. Suzuki, G. Ceder, *Nat. Commun.* **2016**, *7*, 11009.

[134] Z. Zhang, E. Ramos, F. Lalere, A. Assoud, K. Kaup, P. Hartman, L. F. Nazar, *Energy Environ. Sci.* **2018**, *11*, 87.

[135] M. Duchardt, U. Ruschewitz, S. Adams, S. Dehnen, B. Roling, *Angew. Chem., Int. Ed.* **2018**, *130*, 1365.

[136] M. Jansen, U. Henseler, *J. Solid State Chem.* **1992**, *99*, 110.

[137] D. Zhang, X. Cao, D. Xu, N. Wang, C. Yu, W. Hu, X. Yan, J. Mi, B. Wen, L. Wang, *Electrochim. Acta* **2018**, *259*, 100.

[138] A. Hayashi, K. Noi, A. Sakuda, M. Tatsumisago, *Nat. Commun.* **2012**, *3*, 856.

[139] A. Banerjee, K. H. Park, J. W. Heo, Y. J. Nam, C. K. Moon, S. M. Oh, S. T. Hong, Y. S. Jung, *Angew. Chem., Int. Ed.* **2016**, *55*, 9634.

[140] X. Zheng, C. Bommier, W. Luo, L. Jiang, Y. Hao, Y. Huang, *Energy Storage Mater.* **2018**, *16*, 6.

[141] J.-Y. Hwang, S.-T. Myung, Y.-K. Sun, *Chem. Soc. Rev.* **2017**, *46*, 3529.

[142] K. Abraham, Z. Jiang, *J. Electrochem. Soc.* **1996**, *143*, 1.

[143] H. Jusef, C. Fausto, A. Michel, S. Bruno, *Angew. Chem., Int. Ed.* **2011**, *50*, 2999.

[144] E. Peled, D. Golodnitsky, G. Ardel, V. Eshkenazy, *Electrochim. Acta* **1995**, *40*, 2197.

[145] H. Zhang, C. Li, M. Piszcz, E. Coya, T. Rojo, L. M. Rodriguez-Martinez, M. Armand, Z. Zhou, *Chem. Soc. Rev.* **2017**, *46*, 797.

[146] K. West, B. Zachau-Christiansen, T. Jacobsen, E. Hiort-Lorenzen, S. Skaarup, *Polym. Int.* **1988**, *20*, 243.

[147] S. Hashmi, S. Chandra, *J. Mater. Sci. Eng. B* **1995**, *34*, 18.

[148] R. Chandrasekaran, S. Selladurai, *J. Solid State Electrochem.* **2001**, *5*, 355.

[149] B. P. Balaji, M. V. Madhu, S. A. Kumar, R. V. V. R. Narasimha, *J. Appl. Polym. Sci.* **2008**, *108*, 510.

[150] K. N. Kumar, T. Sreekanth, M. J. Reddy, U. S. Rao, *J. Power Sources* **2001**, *101*, 130.

[151] C. V. S. Reddy, A.-P. Jin, Q.-Y. Zhu, L.-Q. Mai, W. Chen, *Eur. Phys. J. E* **2006**, *19*, 471.